Egyptian Journal of Petroleum (2016) xxx, xxx–xxx

HOSTED BY

ELSEVIER

Egyptian Petroleum Research Institute

Egyptian Journal of Petroleum

www.elsevier.com/locate/egyjp
www.sciencedirect.com

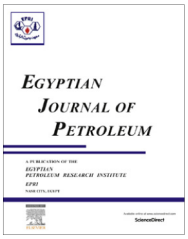

FULL LENGTH ARTICLE

Identify re-development concepts to enhance Abu Roash "C" oil reservoir productivity Sitra Area, Abu Gharadig Basin, Western Desert, Egypt

H. Salama [a,*], **M. Darwish** [b], **M. Wahdan** [a], **A. El-Batal** [c]

[a] *Badr El-Din Petroleum Company (BAPETCO), Egypt*
[b] *Geology Department, Faculty of Science, Cairo University, Egypt*
[c] *Qarun Petroleum Company, Egypt*

Received 28 January 2016; revised 17 March 2016; accepted 13 April 2016

KEYWORDS

Facies modeling;
Depositional model;
Reservoir characterization;
Redevelopment concepts;
Enhance oil productivity

Abstract This study includes a new understanding of the depositional model of Abu Roash "C" Member deposited in Sitra Field in Abu Gharadig Basin during Turonian time, and illustrates the major affecting factors that control the behavior of this reservoir and consequently offer a great opportunity for Sitra field's future development activities through a new methodology to maximize the field's ultimate recovery.

The Sitra development lease is located in north Western Desert and occupies the central western part of Abu Gharadig Basin and covers the southern extension of Badr El-din Petroleum Company (BAPETCO) leases with an area of 322.4 km^2. Sitra Area is divided into several structural closures; the main producing one is the Sitra 8 block in which 39 wells were drilled since 1993. Various data from these wells were evaluated to construct the depositional facies models for the Abu Roash "C" reservoir. The log analyses have been integrated with the core descriptions, and ditch cutting data to interpret the depositional facies model that controlled the reservoir characteristics.

In Sitra Area the Abu Roash "C" Member exhibits all of the characteristics of the Shallow Marine-Tidal dominated estuaries which are linked to the south with a fluvio-marine environment, the tide-dominated estuaries are represented in tidal channels and tidal flat facies, march deposits, and distributary mouth bars. The best reservoir rock in the Abu Roash "C" Member was deposited as distributary channel fill/Mouth bars that cut through the underlying strata.

Two major parasequences were identified, the first lower one was developed during a shallowing upward sequence represented by shale/sand intercalations into which the main Abu Roash "C" reservoir sand bodies are included, and reached its end by the appearance of a laterally extended coal marker nearly one meter thick. This parasequence was deposited subsequently to a falling sea level phase which occurred after the deposition of Abu Roash "D" limestone. The succeeding parasequence (deepening upward) reached its maximum flooding surface (MFS) by the deposition of the widely extensive shale marker being rich in pelagic Pelecypod shells.

* Corresponding author.
E-mail address: H.Salama@bapetco.simis.com (Hanan Salama).

Peer review under responsibility of Egyptian Petroleum Research Institute.

http://dx.doi.org/10.1016/j.ejpe.2016.04.003

Please cite this article in press as: H. Salama et al., Identify re-development concepts to enhance Abu Roash "C" oil reservoir productivity Sitra Area, Abu Gharadig Basin, Western Desert, Egypt, Egypt. J. Petrol. (2016), http://dx.doi.org/10.1016/j.ejpe.2016.04.003

The resultant stratigraphic units consist of: genetically related depositional cycles (3 cycles) and their components of facies sequences (5 facies types), each cycle has its own distribution, facies classification and reservoir characteristics.

1. Introduction

Recently, the most potentially exciting news of Oil and Gas discoveries in Egypt is coming from the Western Desert region, where several outstanding discoveries have been achieved since only eighties [39].

Abu Gharadig Basin comprises many of the most productive oil and gas fields in the northern part of the Western Desert [2]. In Badr El-Din Concession, oil and gas have been produced until now from the Late Cretaceous (Cenomanian - Turonian) Abu Roash C, D, E, F and G Members and from the underlying Cenomanian Bahariya and Albian Kharita formations.

The Badr El Din Petroleum Company (Bapetco) operates the SITRA concession (50% Shell Egypt and 50% EGPC) on behalf of Sitra petroleum Company (SiPetCo).

1.1. Location of the study area

The Sitra development lease is located in the Western Desert and occupies the central western part of Abu El-Gharadig basin and the southern extent of Badr EL-Din concession (Fig. 1). Sitra field has in total six stacked hydrocarbon reservoirs; four reservoirs are located in the Abu Roash Formations in which three of them AR"C", AR"E"& AR"G" Upper are oil bearing and one is gas bearing AR"G" Lower. The last two reservoirs are located in Bahariya Formations, the Upper

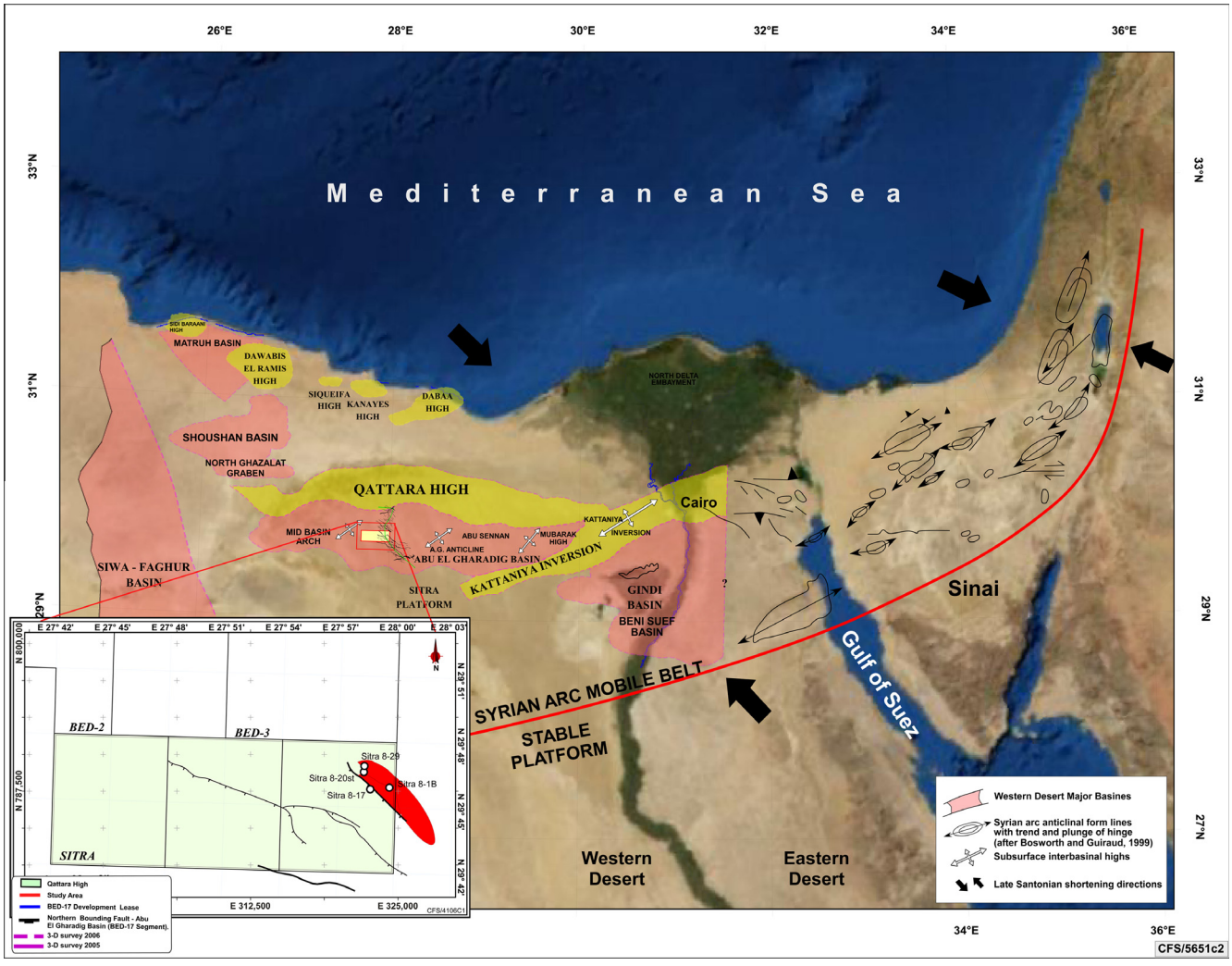

Figure 1 Location maps for Sitra development lease and our study area).

Bahariya is oil bearing while the Lower Bahariya is gas bearing. Kharita reservoir is water bearing.

1.2. The main objectives of this study

- ➢ Integration between core data and Wireline logging data of Abu Roash "C" to identify potentially bypassed HC intervals that might be a way for additional reserves.
- ➢ Facies analyses and depositional model of Abu Roash "C" member.
- ➢ Identify and evaluate alternative re-development concepts for AR"C" oil reservoir through the redistribution of its depositional Model and Facies analyses.

1.3. Previous work

The north Western Desert of Egypt attracted the attention of several workers from the geological and hydrocarbon potential viewpoints. Petroleum potentiality and petroleum systems of the Western Desert have been studied by many investigators, among them are [13,1,10,11,48,59,79,74,83,106,25,64,109,12,93,9,40,41,60,95,33,55,5,2,57,7,54,75,61,62,108], and [63,67,65]. The Upper Cretaceous sequences were the subject of numerous studies since [90]. The surface outcrops at the Bahariya Depression and Abu Roash District were considered the type sections of the Cenomanian-Maastrichtian sequences. The different stratigraphic units of these surface and subsurface sequences were studied by [26,27,51,49,86,87,28,78,44,29,35,36], among others.

The tectonic framework and structural setting of the north Western Desert were studied and analyzed by many authors of mention: [94,86,107,14,83,80,81,70,71], and [72,38,73,3,15,31], and [32,45,66,105].

Previous studies on the Northern Western Desert relevant to the regional integration of the present work include the works of [11,3,104,4,23,43,46,56,42,106,77,6,50,37,30,76].

Cretaceous deposits are widely distributed in the subsurface of the northern Western Desert of Egypt. Since these deposits are major exploration targets for petroleum resources, a lot of palynological work has been done on them e.g. [84,85,97–100, 103,101,102,82,8], and papers cited in [88,89,58].

2. Geologic settings

2.1. Stratigraphic framework of Abu Gharadig Basin

The stratigraphic column in the northern part of the Western Desert is thick and includes most of the sedimentary succession from recent to Pre-Cambrian basement complex (Fig. 2). The Sedimentary cover (i.e. the sequence of deposits overlying the basement rocks) regionally thickens northwards, reaching more than 35,000 ft. in the Abu Gharadig Basin, thinning to some 10,000 feet over the Ras Qattara ridge which marks the northern edge of the basin, [42].

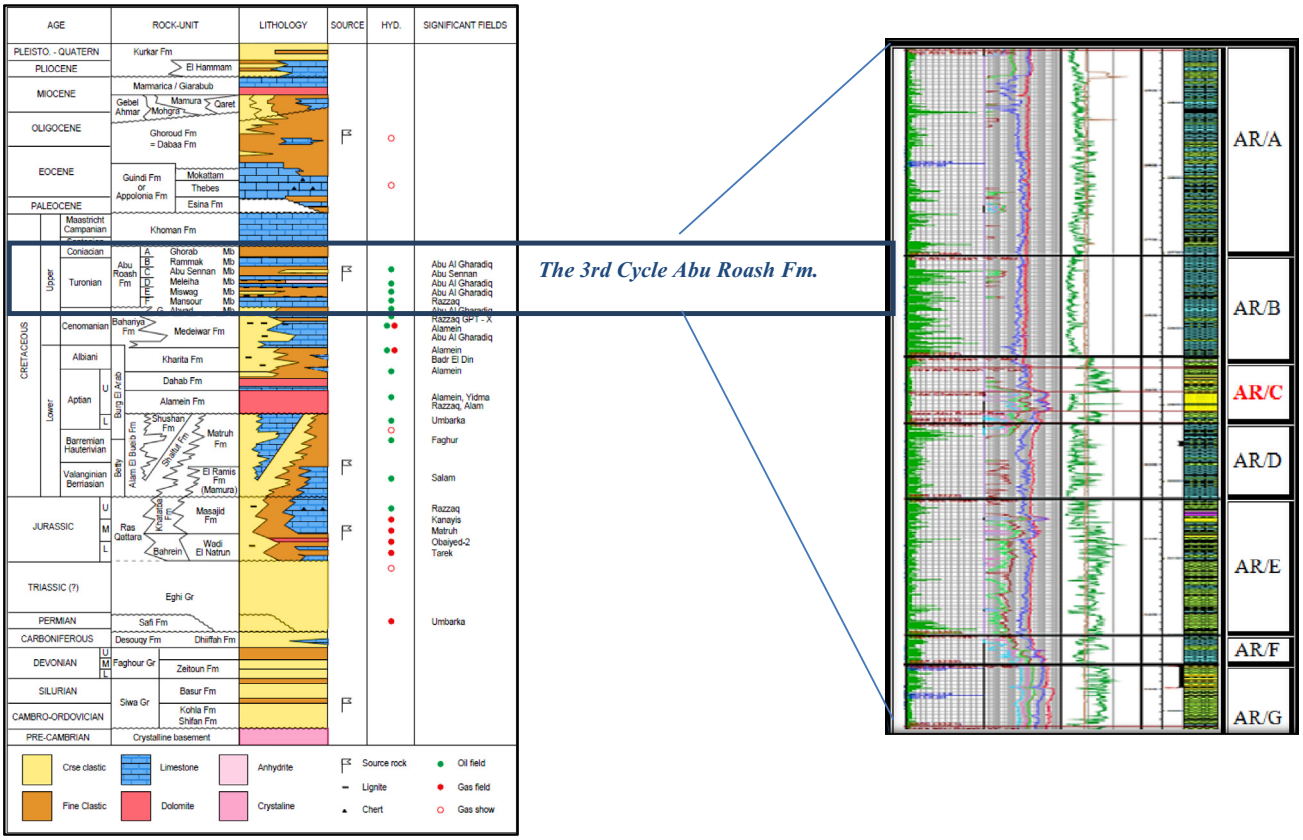

Figure 2 Stratigraphic framework of the Abu Gharadig basin (Modified from WEC Egypt, Schlumberger, 1984; EGPC Western Desert, Oil and Gas Fields, 1992; and O. Shaarawy, GUPCO in M. Abdel Halim, EGPC, 1994).

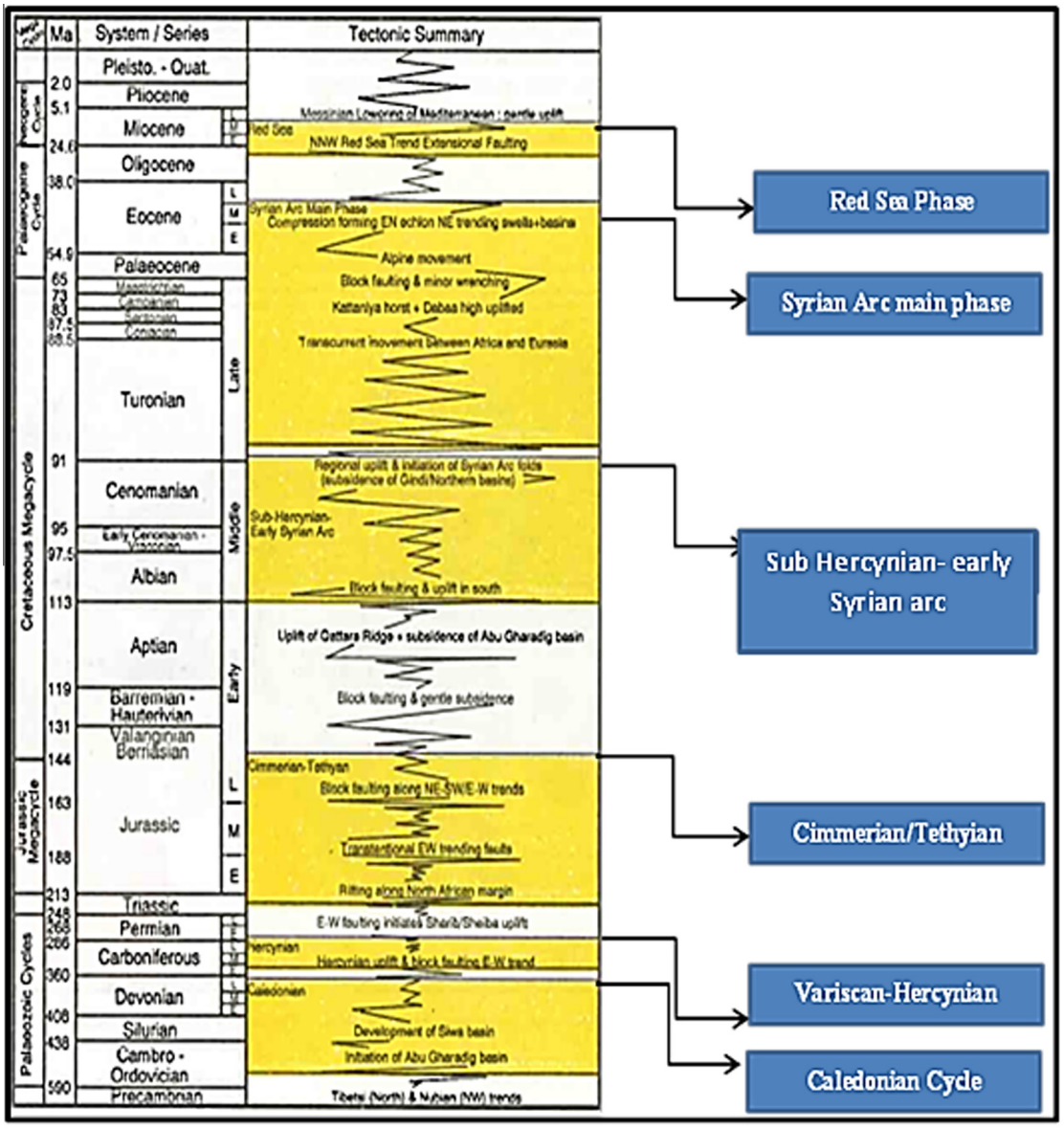

Figure 3 Major Geotectonic cycles, (EGPC, 1992).

The stratigraphic section consists of alternating depositional cycles of clastics and carbonates.

Five cycles have been recognized as follows:

1. The first cycle of clastic facies dominates the oldest sedimentary rocks and includes the entire Paleozoic and Lower Jurassic formations.
2. A carbonate section of Middle and Upper Jurassic formations.
3. The Third Cycle (second cycle of clastics) comprises the Lower Cretaceous up to Upper Cretaceous Early Cenomanian.
4. From Upper Cenomanian and up to the Middle Eocene, dominant carbonate deposits are again distributed throughout northern Western Desert.
5. The upper most clastic depositional cycle includes the Upper Eocene–Oligocene, Miocene and younger section.

There is evidence over much of the Western Desert that the upper boundary of the Abu Roash Formation is an unconformity. Abu Roash Formation thickens to the north and becomes dominated by carbonates in the Mediterranean coastal area.

It has Cenomanian to Turonian age, locally extending into Coniacian and Santonian in the upper most units (“A” and “B”). The Abu Roash Formation was deposited on a wide shallow marine shelf during several sedimentary cycles, in response to oscillation of the sea level. Transgressive phases are marked by limestone and shale sequences, while regressive phases are clastic dominated.

Fully Marine conditions persisted throughout the Late Cretaceous and the Paleogene. The Upper Cretaceous Abu Roash and Khoman formations are characterized by a cyclic alternation of shallow water sandstones, neritic to deep-water Limestones, and deep-water Shale. The transgressive/regressive

sedimentary cycles of the Abu Roash Formation are regionally important and have been labeled the "A" Member, at the top, through to the "G" Member at the base. The "A", "B", "D", and "F" Members are mainly composed of carbonates and shale, deposited in a neritic environment, while the Abu Roash "C", "E", and "G" Members contain coastal plain, lagoonal, and shallow marine sands and shales, together with some thin limestones. All of these sands have potential reservoir quality, and are Oil-bearing in several fields in Abu Gharadig Basin [24].

The Abu Roash Formation has been divided into seven units "A" to "G", "A" was being the highest. Units "B", "D" and "F" are relatively clean carbonates, units "A", "C", "E" and "G" contain variable amounts of detrital material. The Lower boundary is at the base of Abu Roash "G" which rests on the Bahariya Formation. The upper boundary of the Abu Roash is the base of the Khoman Formation or of the Apollonia Formation, whenever the Khoman Formation is missing.

2.2. Tectonic framework

The tectonic evolution of northeast Africa has been extensively described by numerous authors (including [86,72]). Several continental plate collision phases are recorded between Pangea mega segments of Laurasia and Gondwana throughout the

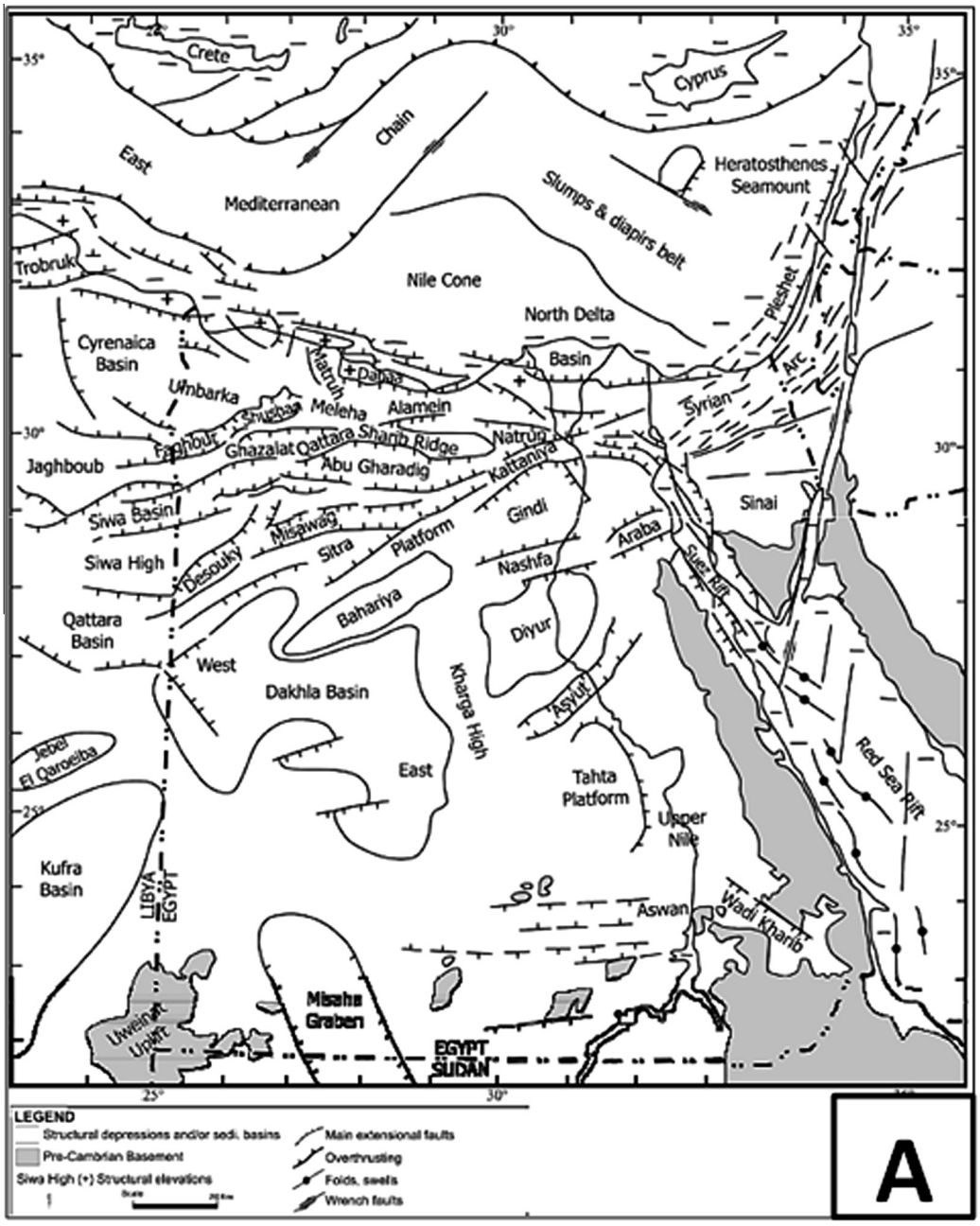

Figure 4 (A) Map of Egypt and southeast Mediterranean Sea showing main structural elements and sedimentary basins (modified after [Sestini, 1995]). (B) Basement tectonic map of North Western Desert (after Meshreif, 1988).

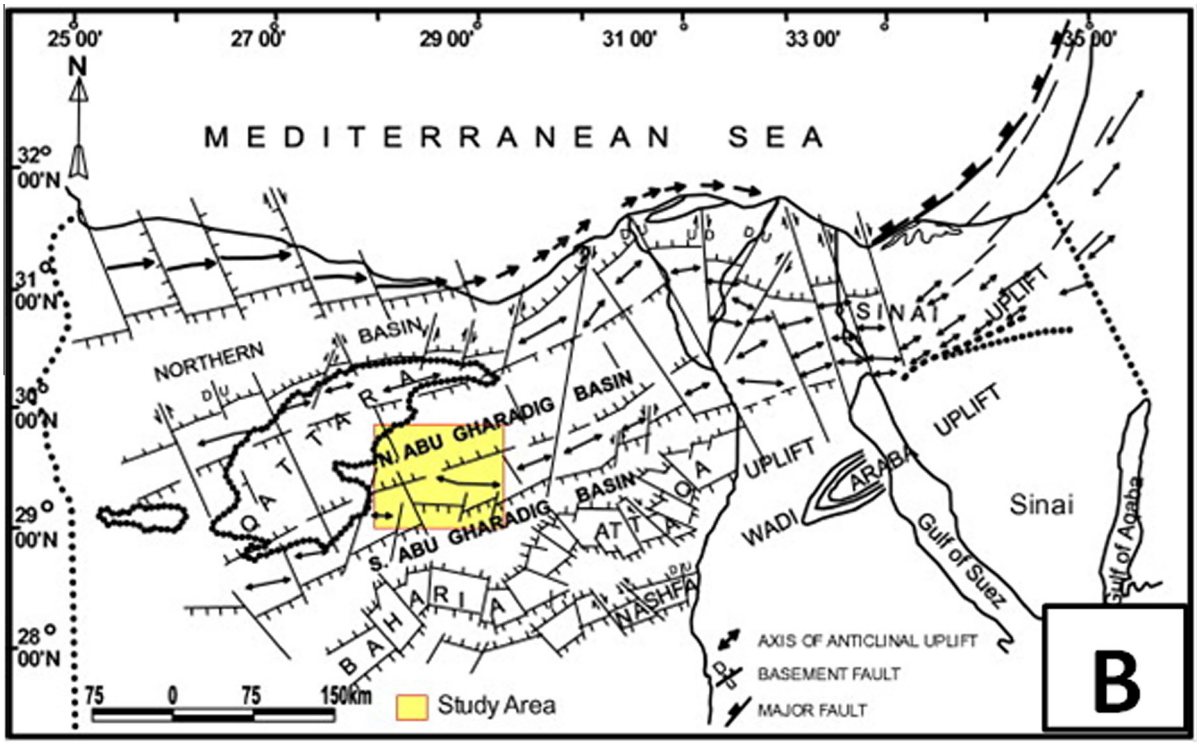

Fig. 4 (*continued*)

Phanerozoic [92]. Late Carboniferous to early Permian rifting and crustal separation was the first step in the break-up of Pangaea with the opening of the Permo-Tethyan seaway and the East Mediterranean Basins.

These were interrupted by extensional rift phases associated with oceanic crust formation and flooding of continental plate margins. A further important factor was the sinistral or dextral rotation of the Sahara/North African plate relative to Laurasia, which had a strong modifying effect on the local basinal tectonic styles encountered in the northeast Africa and in particular the Western Desert.

Egypt lies at the northeastern corner of the African plate and can be broadly divided into four structural divisions. These are the Hinge Zone and Unstable Shelf in the north, and the Stable Shelf and the Nubian/Arabian Cratons in the south [86]. The Stable Shelf is a belt extending from southern Egypt to a northern limit arriving as far as central Sinai. It is characterized by low structural relief and with thin sedimentary cover of fluvio-continental deposits mainly of Mesozoic age, deformed by several sets of regional folds [86]. The Unstable Shelf occupies almost all of the northern parts of Egypt, characterized by a northward thickening sedimentary section underlain by high basement relief due to block faulting. Moreover, it is characterized by surface tectonic features of lateral stresses due to different compressional episodes such as Syrian Arc folds in northern Sinai.

On the other hand, the Hinge Zone coincides nearly with the present Mediterranean coastal area separating the unstable shelf from the Miogeosynclinal basinal area. It causes a rapid, basin wards thickening of Oligocene to Pliocene sediments. Presently it is submerged and partially buried under thick Plio- Pleistocene deposits in relation to the Nile Delta.

On the other hand, Egypt can be subdivided into five major morpho-structural units (Fig. 4(A)). (1) the Mediterranean Fault Zone, (2) a belt of linear uplifts and half-grabens, (3) the North Sinai Fold Belt "Syrian Arc", (4) the Suez and Red Sea Graben, and (5) the intra-cratonic basins of southern Egypt.

The Central portion of the Western Desert covers the transition zone between the Stable and the Unstable Shelves. Six major geotectonic cycles or phases can be recognized in the Phanerozoic in the Western Desert these are (Fig. 3):

1. Caledonian Cycle (Cambrian-Devonian)
2. Variscan-Hercynian (Late Paleozoic)
3. Cimmerian/Tethyian (Triassic- Early Cretaceous)
4. Sub-Hercynian-Early Syrian Arc (Turonian Santonian)
5. Syrian Arc main phase (Paleogene)
6. Red Sea Phase (Oligocene–Miocene)

Structurally, Abu Gharadig Basin is primarily extensional in nature and is affected mainly by faulting. Folding is relatively subordinate and is often related to movements on nearby faults. Abu Gharadig anticline appears to be related to the Syrian arc system, which is comprised of a series of NE–SW trending folds that cross the entire unstable shelf of northern Egypt. This system has been attributed to Late Cretaceous-Early Tertiary NW–SE compression (normal to the folding axis). The structural style of the Abu Gharadig anticline is proposed to be the result of a regional east–west right lateral shear couple. The structure is a northeast plunging asymmetric anticline which has been cut by a series of northwest trending extensional faults. These faults have dissected the field into a number of separate reservoir blocks. [42,70–73] studied the tectonic

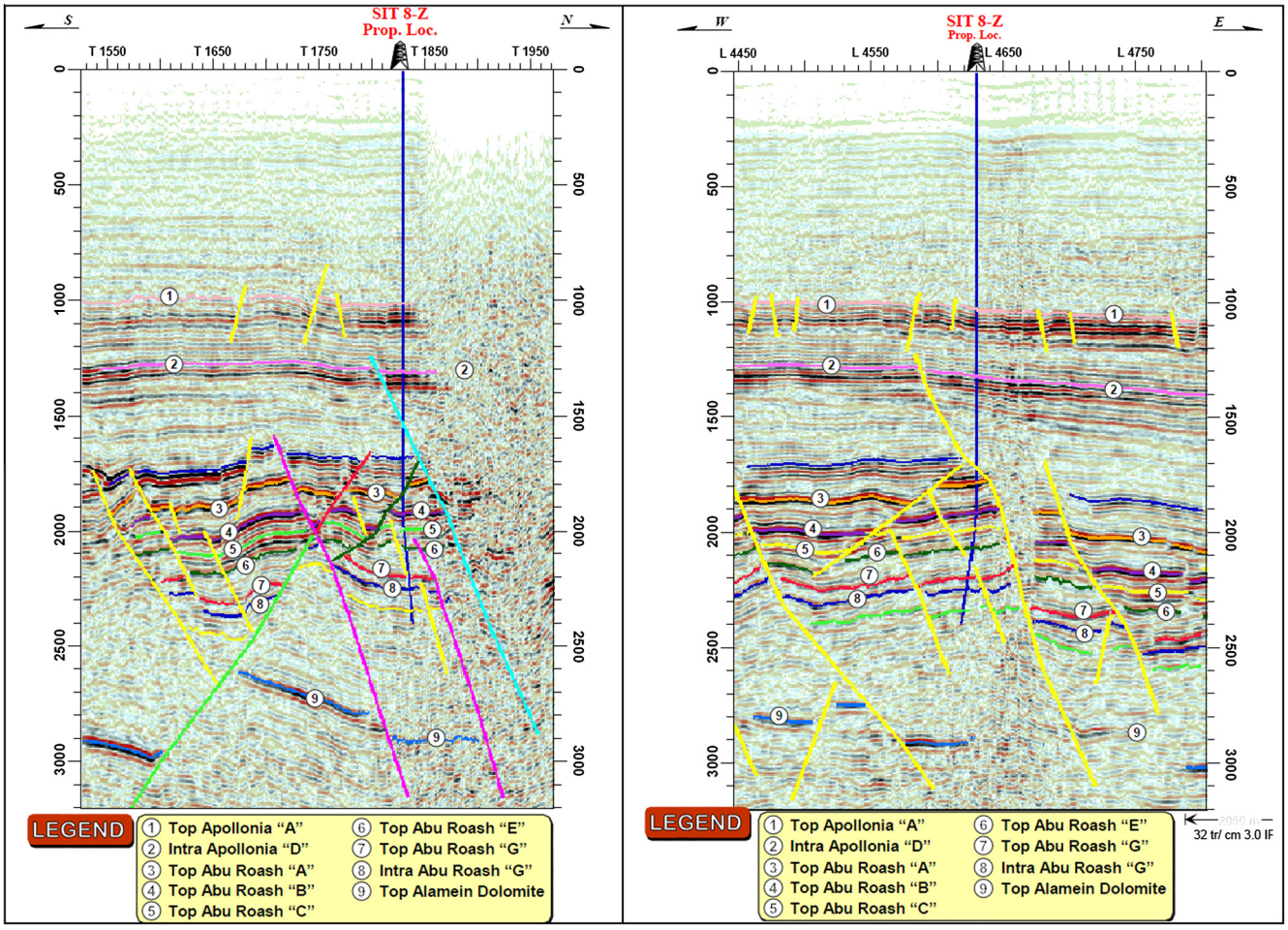

Figure 5 N–S Seismic (Trace 4618) passing through Sitra 8-29(Z) to the left, E–W Seismic (Line 1839) passing through Sitra 8-29(Z) to the right (After BAPETCO Geophysics team, 2012).

trends in northern Egypt using the potential data and suggested several uplifted structures separated by ENE trending basins. He concluded that the E–W and N 65° E (Syrian Arc) trends are more developed in the northern Western Desert (Fig. 4(B)). The northern anticlinal structures are extended on-land at the extreme western portion of the northern Western Desert. Southwardly, this trend is followed by the Qattara-north Sinai uplift, Bahariya–Ataqa uplift and Nashfa-Wadi Araba uplift.

3. Materials and methodology

3.1. Data set and data quality

- The available well data of only four wells in the study area (Surface location coordinates (Red Belt system); Deviation data; Log data (conventional logs and calculated curves); and Formation tops).
- The available Electric logs (Gamma Ray, Density, -Neutron, and Resistivity logs).
- 20 seismic lines (2D and 3D) as a hard copy.
- Available Geologic reports (Core reports, Biostratigraphic reports, final well reports. . .etc.).

3.2. Methodology

3.2.1. Geophysical data

The evaluation work was carried out within two phases

i. The first phase: The evaluation work was carried out on the PSTM processed 3D 2008 seismic data.
ii. The second phase: The evaluation work (more fine-tuned work) was carried out on the PSDM processed 3D (2010/2011) seismic data.

In the Sitra Area (like most areas in the Western Desert) the seismic attributes are not a clear indicator of sand or hydrocarbon presence, though investigation should continue in support of the subsurface analysis.

3.2.2. Geological data

3.2.2.1. Lithofacies analysis.

➢ Detailed lithologic description of the individual lithofacies units identified on the core slabs with emphasis on lithologic composition, bed thicknesses, color, grain-size arrangement patterns and degree of crystallinity for detrital and authigenic components respectively, vertical grain size

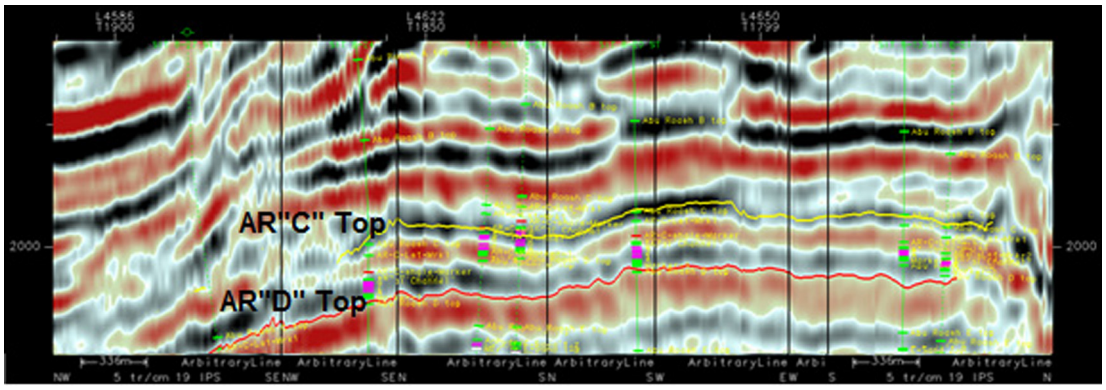

Figure 6 Arbitrary line passing through Sit 8-29 and Sit 9-20 St. with more focusing on AR "C" seismic marker.

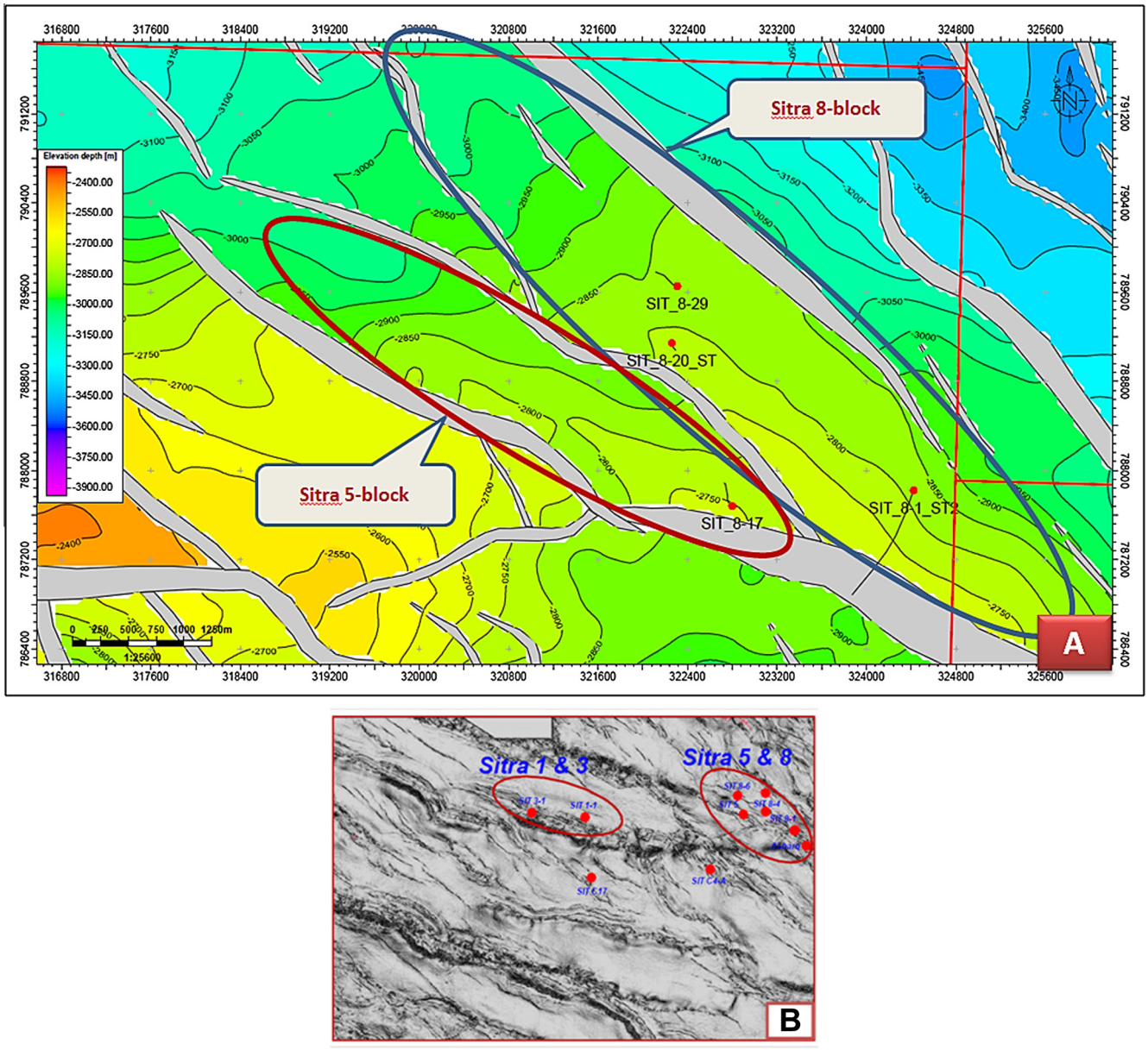

Figure 7 (A) A/R "C" seismic marker structure map (B) A/R "C" semblance map.(After the geophysics team in BAPETCO, 2014).

Table 1 Available well data.

Well name	Mud logs	Electric logs	Core data	Image data (BHI)
Sitra 8-1 ST2	√	√	√	×
Sitra 8-17	√	√	√	√
Sitra 8-20 ST	√	√	×	×
Sitra 8-29	√	√	×	×

profiles, primary sedimentary structures, biogenic features (body and/or traces), mineralogical aspects, bed contacts, truncation events and/or erosional surfaces and hydrocarbon indications.

➢ Plotting of the above-mentioned data on working sheets at a scale of 1:10. These sheets are then used in compiling sedimentologic log charts (scale 1:40) showing a graphical representation of the various depositional aspects and pertinent data plotted against the gamma-ray log of the cored succession, routine core analysis data and plain-light and ultraviolet-light photographs of the slabbed core surfaces. These charts show the subdivision of the cored successions into their component lithofacies with a text description for each.

➢ The identified lithofacies suit is then used to diagnose the depositional environment of studied succession and accordingly to predict the geometry of the significant lithofacies units.

3.2.2.2. Thin-section petrographic analysis. Petrographic investigation of blue dye-injected thin sections were prepared from selected core chips and examined under a research-grade polarizing microscope. The investigation focuses on determining the mineral composition, matrix and/or cement material, fabrics and textures, porosity type(s) and degree of connectivity and syn- and post-depositional modifications. On determining the petrographic clans to which the analyzed samples belong, the sandstone classifications and carbonate rock classification schemes were applied.

3.2.2.3. Scanning-electron microscopy (SEM). Scanning electron microscopy involves bombardment of gold-coated raw surfaces of the rock specimens by low velocity electron beams which upon reflection yield detailed surface morphology at

Table 2 Core data of the available wells.

Well name	Core No.	Cored interval without shift		Core shift	Recovery (%)	Length Per Core	Cored interval with shift		Formation
		Top (mbdf)	Bottom (mbdf)				Top (mbdf)	Bottom (mbdf)	
Sitra 8-1B	Core #1	2940.50	2959.00	6.5+	100%	18.50	2947.00	2965.50	A/R "C"
	Core #2	2959.00	2977.00	6.8+	100%	18.00	2965.80	2983.80	
Sitra 8-17	Core #1	2837.17	2864.23	0.23+	100%	27.06	2837.40	2864.46	A/R "C"

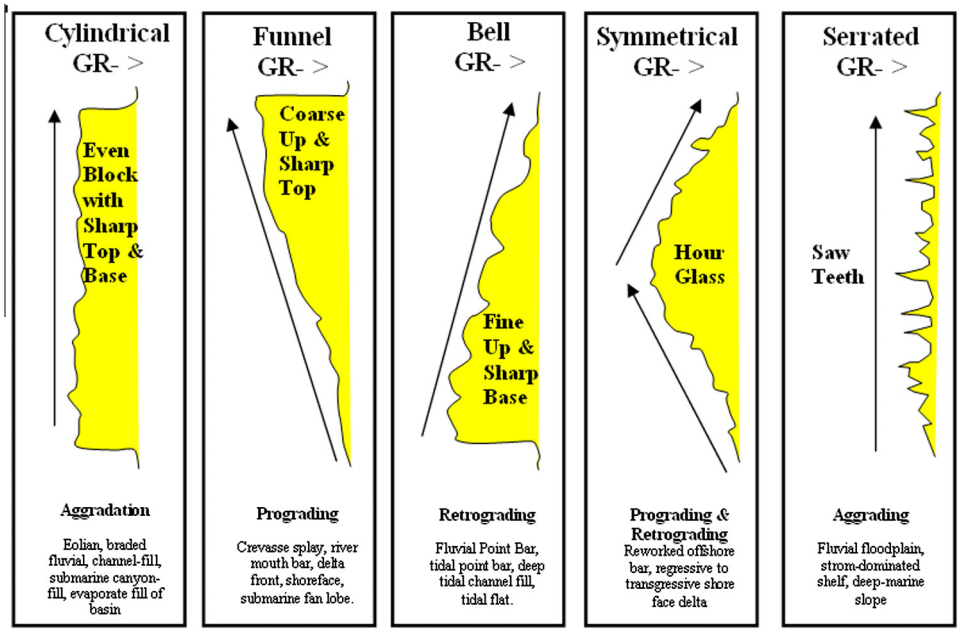

Figure 8 The direct correlation between facies and a variety of other log shapes relative to the sedimentological relationship (Cant, 1992).

nanometer scale. SEMs are capable of obtaining images at magnifications over 100,000 times. These instruments can see and then analyze something that would not show up with a polarized-light microscope.

3.2.2.4. X-ray diffraction (XRD) analysis.

- ➢ This was carried out both for the bulk-samples and for their clay fractions.
- ➢ For the bulk-sample examination, the samples were preliminarily investigated under the binocular microscope for determination of their gross characteristics and texture, and were then X-rayed for determination of their gross mineralogy.
- ➢ For the clay fraction examination, the clay fraction is prepared through crushing a part of the bulk sample, plunging it with water, letting it settle down and pipetting a part of the suspension after certain period of time estimated so that the suspended material is made up of less than 2 μm size. This is the size that is richest in clay minerals with the possibility of co-existence of particles of other minerals.

3.2.2.5. Biostratigraphic analysis. The high resolution biostratigraphic analyses are based on the frequency and abundance of the identified taxa supported the biozonation and environmental interpretation for the studied succession.

Sitra 8-29 : the largest sand thickness represent a blocky pattern of the main tidal channel coming from the north

Sitra 8-20 ST: a group of stacked channels represented by a fining upward and blocky patterns

Sitra 8-b ST2: a very clear fining upward pattern in the stacked channels

Sitra 8-17 Two types of deposition , a clear coarsening upward pattern represented by the deposition of the mouth bars at the lower part and fining upward pattern for the tidal channel above the coal marker

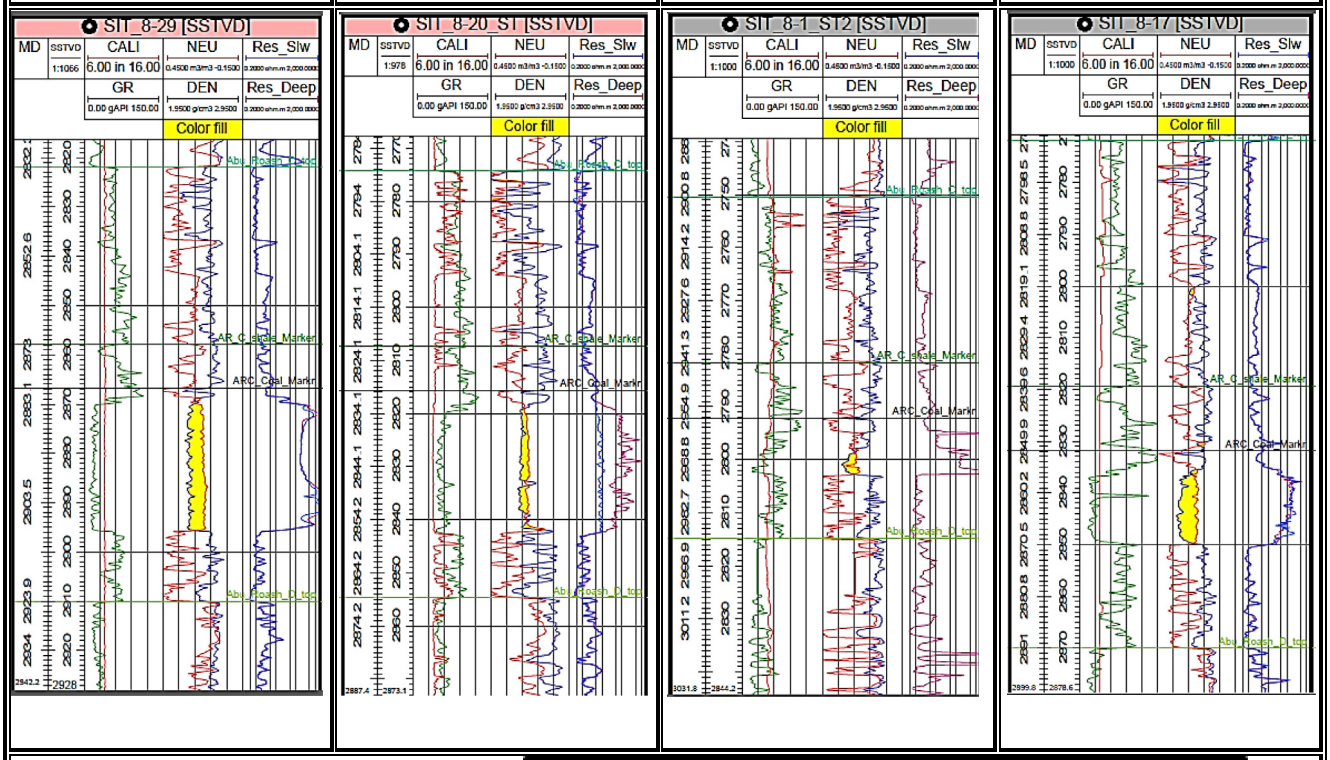

Legend:

- AR"C" Top
- AR"C" Shale Marker
- AR"C" Coal Marker
- AR"D" Top

Block no.	Well NAME	ARC			
		Top (TVDSS)	Bottom (TVDSS)	Gross thickness (m)	Net Sand (m)
Sitra 8 block	Sit 08-1 St2	2750	2815	65	5
	Sit 08-20 St	2774.4	2854.8	80.4	20.5
	Sit 08-29	2822	2910	88	31
Sitra 5block	Sit 08-17	2771.9	2870	98.1	16

Figure 9 Well logs from N to S respectively; reservoir interval lies under the AR "C" shale marker in all wells.

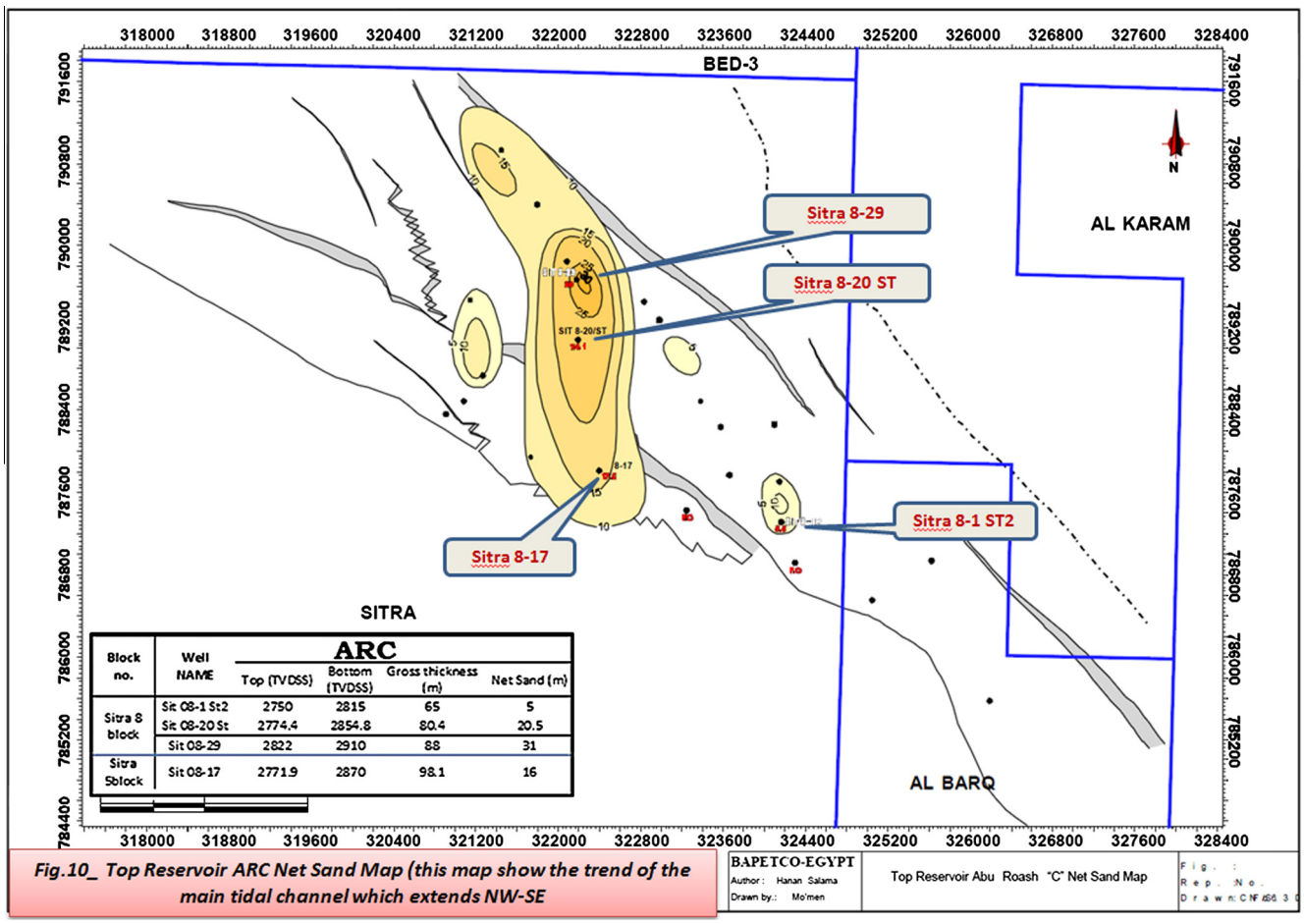

Figure 10 Top Reservoir ARC Net Sand Map (this map show the trend of the main tidal channel which extends NW–SE.

Table 3 Petreophysical data and calculations.

Block No.	Well NAME	AR/C						
		Top (TVDSS)	Bottom (TVDSS)	Gross thickness (m)	Net Sand (m)	Net/ Gross	Porosity % (Fig. 12)	Saturation SW %
Sitra 8 block	Sit 08-1 St2	2750	2815	65	5	0.078	22%	45
	Sit 08-20 St	2774.4	2854.8	80.4	20.5	0.255	17.6	16
	Sit 08-29	2822	2910	88	31	0.352	19	10
Sitra 5 block	Sit 08-17	2771.9	2870	98.1	16	0.163	21%	48

4. Results

4.1. Seismic interpretation

The evaluation work (more fine-tuned work) was carried out on the PSDM processed 3D (2010/2011) seismic data. The seismic interpretation was carried out for three horizons and well to seismic matches were done using the Sitra 8 & SITRA 5 wells.

- Top Abu Roash "C"
- Intra Abu Roash "G" Limestone
- Top Alamein Dolomite

"Top A/R "C" reflector represents an acoustically hard to soft transition (soft kick) and it is displayed on the workstation as (positive) black loop".

The AR"C" channel sand in the northern part of the Sitra 8 structure reaches its maximum thickness at the Sitra 8-Z (29) location. In the Sitra Area (like most areas in the Western Desert) the seismic attributes are not a clear indicator of sand or hydrocarbon presence, though investigation should continue in support of the subsurface analysis. Current understanding is that no direct hydrocarbon indicator from seismic exists in the "Greater BED & Sitra" areas. The explanation is attributed primarily to the quality of the seismic data (Figs. 5 and 6).

Please cite this article in press as: H. Salama et al., Identify re-development concepts to enhance Abu Roash "C" oil reservoir productivity Sitra Area, Abu Gharadig Basin, Western Desert, Egypt, Egypt. J. Petrol. (2016), http://dx.doi.org/10.1016/j.ejpe.2016.04.003

4.2. Structural interpretation (incl. TD conversion)

Sitra development lease is dominated by a series of narrow elongate East–West trending horsts and grabens. The known hydrocarbon accumulations are trapped in the sandstone reservoirs of the Bahariya and Abu Roash formations. The Sitra 5 & 8 structure is adjacent to the large SIT 1-1/3-1 WNW to ESE plunging structural nose. The NW–SE trending orientation of the Sitra 5 & 8 closure and faults is very similar to the main structural trends observed in the area. At A/R "C" level the Sitra 5 & 8 closure is bounded and dissected by several NW-SE trending faults resulting in an accumulation with several (isolated) compartments as shown in (Fig. 7).

The Sitra 5 area represents the crestal part of the Sitra 5/8 structure. However, the hydrocarbon distribution and contacts observed in both the Sitra 5 and 8 fields suggest that the two accumulations are separated by the NW–SE trending North dipping fault [22].

4.2.1. Sitra 1 & 3 field

The Sitra 1 and Sitra 3 fields were evaluated using the Pre-stack Time Migrated data as a 3-way dip closure bounded to the south by a WNW-ESE trending fault. There is no crestal penetration at the at A/R "C" level (Sitra 3-1 faulted out) and crestal appraisal is required [22].

4.3. Depositional environment and facies classification

In this study four wells have been chosen and evaluated based on the main depositional direction in the area (NW–SE), and for more accurate results two of these wells have cores in the Abu Roash "C" member (Sitra 8-1 ST2 and Sitra 8-17).

The depositional environment and conceptual model of the A/R "C" in Sitra Area were derived from cored intervals and Well logs of the available wells (Table 1).

4.3.1. Core data

(Table 2).

4.3.2. Wireline logging data

4.3.2.1. Well logging analysis. The following illustration is used for the facies interpretation from well logs (Fig. 8) [96].

GR and NEU/DEN wireline logs show that sand channels have a sharp erosive base and have a blocky (clean sands) or fining upward pattern (possible channel abandonment) in case of tidal channels with locally serrated shape (more heterolithic), and a coarsening upward pattern in case of deposition of the distributary mouth bars (Sitra 8-17). (Fig. 9). After interpreting the top and base of AR"C" member a net sand map was constructed to show the net sand thicknesses in the area and the trend of the deposition (Fig. 10) [16,18–20].

4.4. Petrophysical evaluation

Porosity Determination

- Porosity was determined based on the density log using the following model:

$$\phi = \frac{\rho_m - \rho_b}{\rho_m - \rho_f}$$

ρ_m; Matrix density ρ_f; Fluid density

ρ_b ; Bulk density

Water Saturation

- Archie's model is used for hydrocarbon saturation calculation. Density-porosity and deep resistivity are used as input for Archie's model using the following equation.

$$s_w = \sqrt[n]{\frac{por^m * R_t}{R_w}}$$

R_W: Formation water resistivity R_T: Deep resistivity

m: Cementation exponent n: Saturation exponent

Formation	ρ_m	ρ_f	Rw	m	n
AR_C	2.67	0.8	0.043	2	2

Net Sand Definition; The method used to define the net sand is neutron-density crossover, manual picking was also used for sand intervals based on other logs like PEF (Photo-Electric Effect) and well cuttings due to encountered high washouts.

4.4.1. Petrophysical calculations

(Table 3).

4.4.2. Permeability estimation

The permeability was estimated for the A/R "C" based on the available core data in SITRA Area in A/R "C",

A/R "C"

The permeability was estimated based on the core data in well SIT8-1B. Log derived permeability calculated in this way was found over estimated comparing with the production data. Three sand facies were defined (see Fig. 11) and based on these facies three transforms were defined and used to estimate the permeability.

4.4.3. Petrophysical properties and results

Sums and averages have been calculated using methodology discussed above in addition to below comments:

- Net sand counts are based on a lithology (VSH) cut-off only (VSH cut-off of 50%). Cemented intervals have been eliminated (manually) based on neutron/density cross-over (to decrease the uncertainty of (net/gross) ratio). No other cut-off for porosity and saturation has been applied for the net PAY definition. Net pay is defined using an additional water saturation cut-off of 50%.

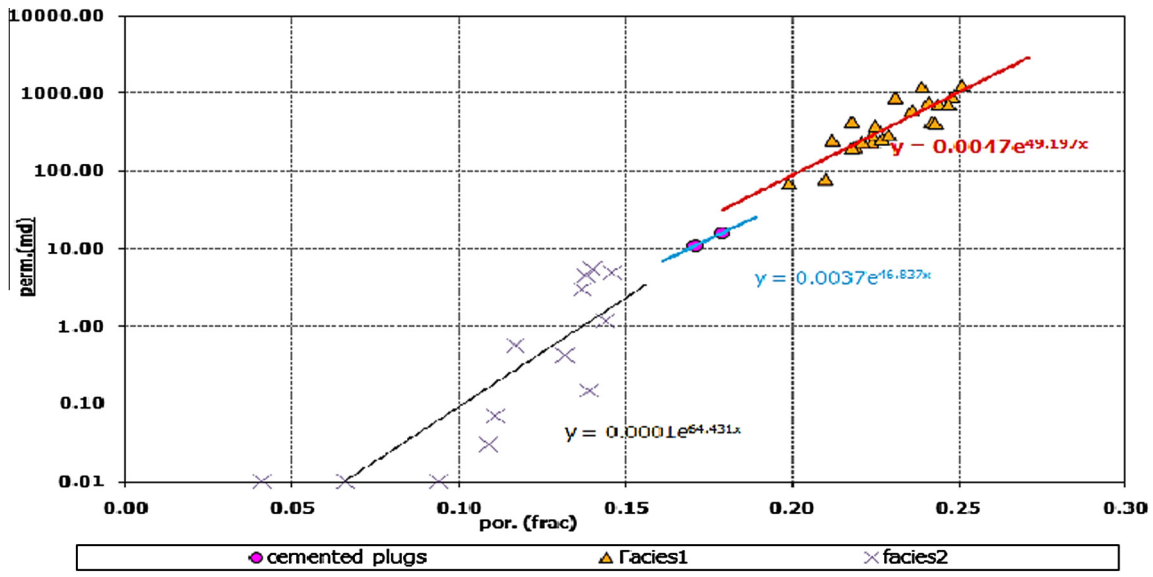

Figure 11 Por-Perm relationship per facies of ARC in well sitra 8-1B.(Facies 1: clean sands (massive/cross bedded), Facies 2: heterolithic/shaly facies.

Table 4 Sums and averages for Abu Roash "C" member.

ARC	Thickness type	Sum	Ave.	P10	P50	P90
	Gross thickness	331.5	82.875	65	81.6	98.1
	Net sand	71.5	17.875	5	18	31

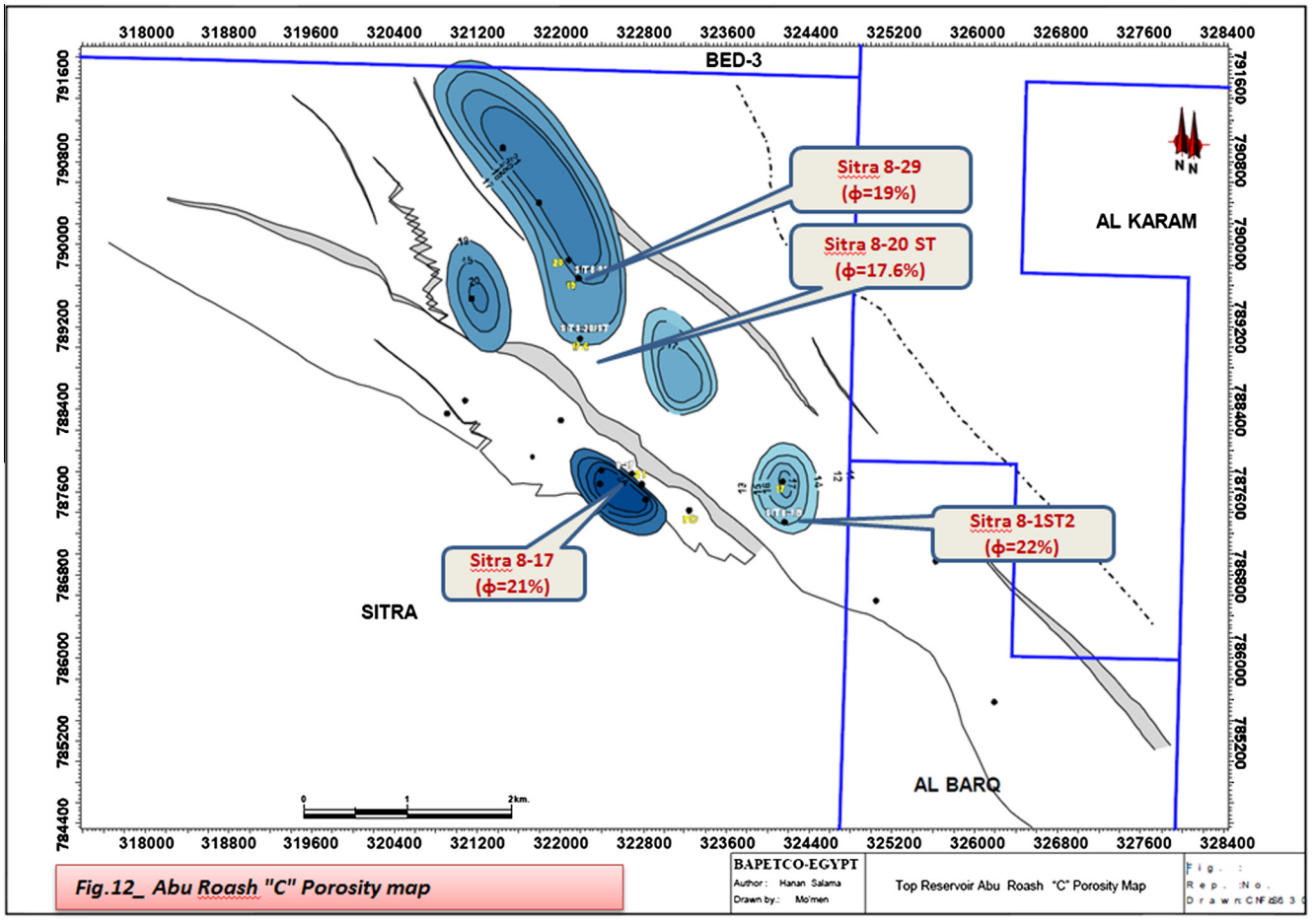

Figure 12 Abu Roash "C" Porosity map.

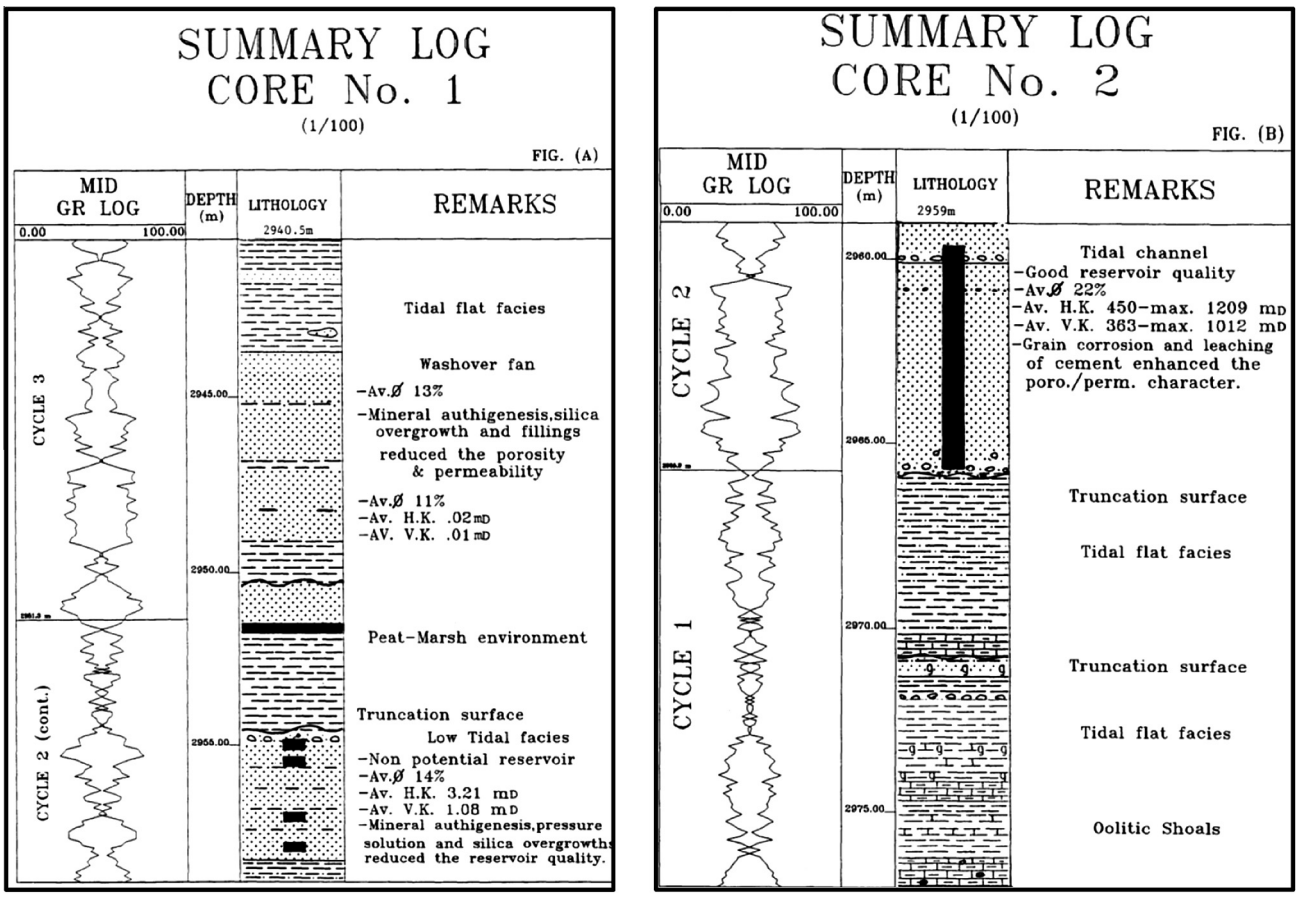

Figure 13 Summery log of the cored intervals Core No. 1 to the left and core No. 2 to the right.

- ➢ Net reservoir is calculated mainly based on Vsh < 50% to be considered as reservoir, in addition to removal of invalid data against the washout intervals.
- ➢ Net Pay is calculated using Sw < 50%.
- ➢ Sums and averages for Abu Roash "C" member are given in Table 4.
- ➢ Porosity distribution in the study area (Fig. 15).

4.5. Facies classification

The study of tidal processes and modern and ancient tidal depositional systems has resulted in a comprehensive suite of diagnostic criteria for the recognition of tidal deposits, particularly at the scale of primary sedimentary structures, bedding styles and facies characteristics, including their biological aspects (e.g. [91,69]; for historical reviews).

From the detailed analysis of the Cored intervals of Abu Roash "C" member we can easily classify this formation into a number of facies depending of the lithological combinations, primary structures, and biological contents.

4.5.1. Sitra 8-1 ST2:[16,21]

The examined samples from Bapetco's Sit 8-1B well core No. 1 (2940.5–2959 mbdf) and core No. 2 (2959–2977 mbdf) are composed of siliciclastic rocks (sandstone, mudstone and shale) with thin carbonate interbeds near the base. The section includes the Oil-bearing sandstones at depth 2955–2965.95 mbdf of the Abu Roash "C" Member that represents the tidal channel cutting in the underlying lagoonal to tidal flat shales.

The oil bearing interval could be subdivided into a lower potential oil bearing reservoir (2959.6–2965.95 mbdf), overlain by tight, less potential argillaceous sandstones with scattered oil saturations.

The potential oil bearing sand stone reservoir is characterized by good to excellent reservoir quality. It has a measured helium porosity in the range between 17.1% and 25.1%, average 22%, and a measured permeability, H.K. 10.9–1269 mD with an average 450 mD and V.K. 2.28–1012 mD, with an average 363 mD. The petrophysics parameters are getting better with depth in the oil bearing sandstone.

The non-potential reservoir has a lower porosity, ranging between 13.7% and 14.6%, average 14%, measured horizontal permeability between 0.14 and 5.52 mD, average 3.22 mD and a vertical permeability 0.17–2.58 mD with an average 1.08 mD. The noticeable permeability decrease is due to the increase in argillaceous matrix, mud streaks and the thin laminations of the sandstone body.

The cored intervals represent a complex domain of shallow marine intertidal facies, partly emerged to marsh conditions which was marked by the accumulation of a thin coal marker.

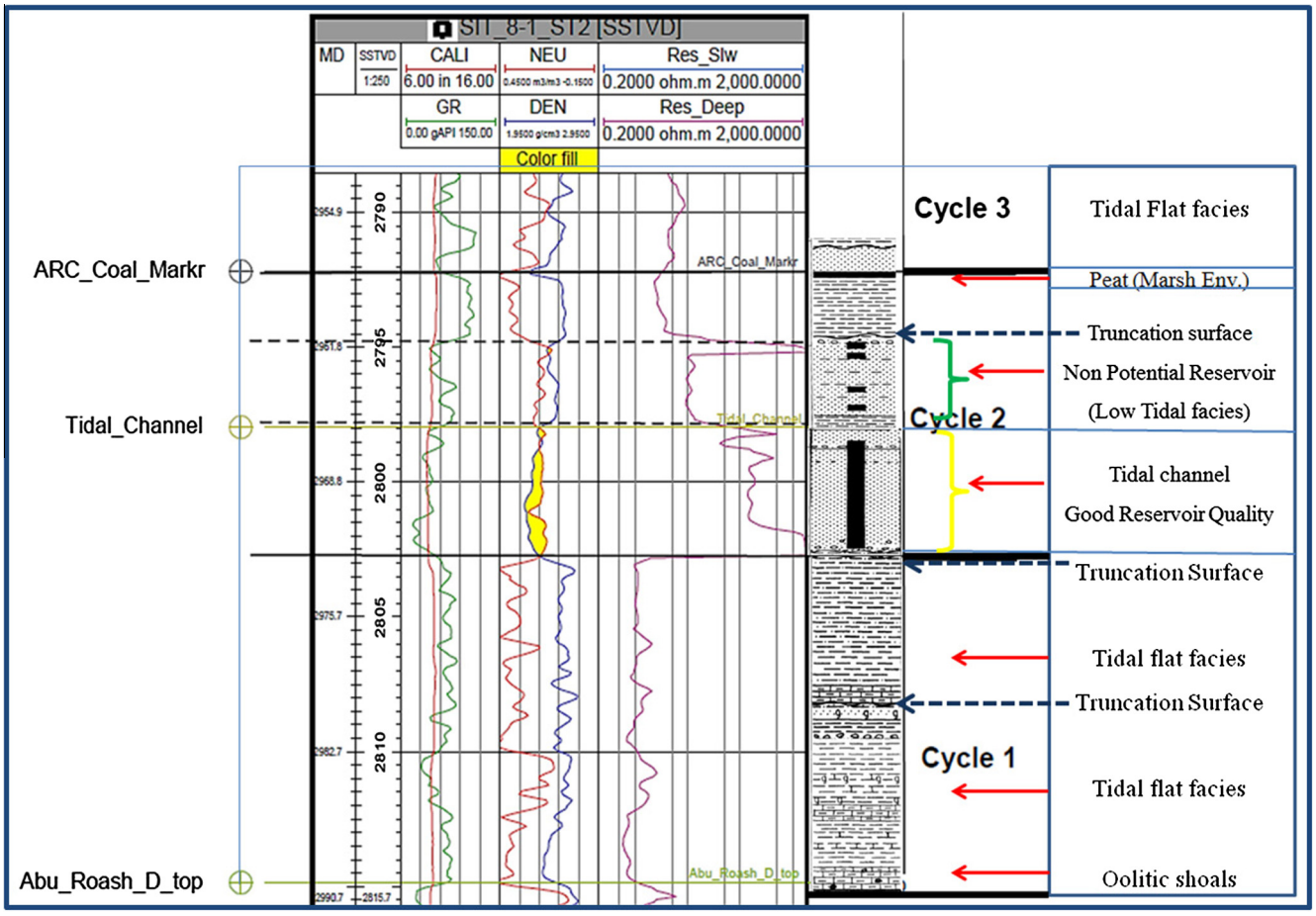

Figure 14 Facies classification according to the cored interval of Abu Roash "C" in (Sitra 8-1 ST2) well.

Table 5 Abu Roash "C" member Facies classification.

Facies	Lithology	Thickness (m)	Environment	Comment
5	Shale/Limestone/Siltstone	35	Marine	Deepening Upward
4	Very fine sandstone	5	Tidal flats	Burrows, flaser bedding, mud cracks
3	Coal	1	Swamp/Marsh	
2	Sandstone	10	Tidal Channels/Mouth bars	Main Reservoir Good Reservoir Quality
1	Shale/Silt/Oolitic shoals	24	Lagoon/Brackish bay	Brackish water

Tasble 5-Sedimentological characteristics of the Abu Roash "C" member (according to Bayoumi, 1994) Thichnesses are taken from well Sitra 8-1 ST2.

Three main depositional cycles are recognized. These are from base to top (Figs. 13 and 14).

- Cycle 1: Carbonate/mudstone/shale capped by a major truncation surface (2977–2965.95 mbdf).
- Cycle 2: Channel sandstone (oil bearing)/shale and terminated by a coal bed.
- Cycle 3: Sandstone and shale (upper limit is incomplete) (2951.35–2940.5 mbdf).

Six depositional environments are encountered from base to top as follows:

- Oolitic ramp margin i.e. shoals (base of Cycle 1).
- Back lagoon to shallow subtidal regime (Facies A and C)
- Tidal channel (Facies A_1) and low tidal sand flat (Facies A_2)
- Marsh (Facies D), end of Cycle 2.
- Strand beach or wash over fan (Facies A) middle part of Cycle 3.
- High tidal flat (muddy facies) at the end of Cycle 3.

4.5.1.1. Facies scheme. The examined cores revealed the dominance of siliciclastics with subordinate carbonate facies. Minor occurrence of coal streaks and one bed are also present.

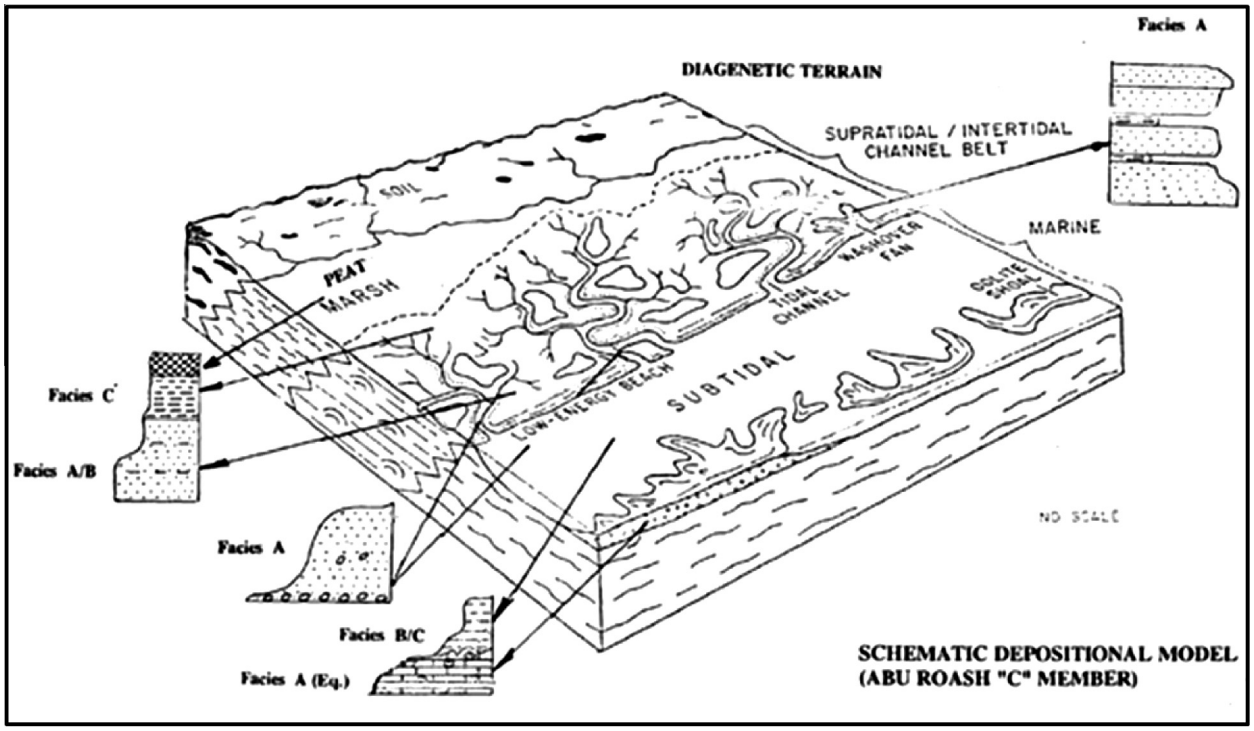

Figure 15 Schematic Depositional model for Abu Roash "C" Member derived from Sitra 8-1 ST2 core description.

Table 6 Interpretation of the lithofacies analysis and depositional environment.

Lithology Type	Lithofacies Code	Explanation
Coal	C	Coal
Conglomerate	Gms	Matrix-supported conglomerate
Sandstone	Sm	Massive Sandstone
	Shl	Flat Laminated Sandstone
	Sb	Bioturbated Sandstone
	Swf	Wavy Laminated Sandstone with Mud Flasers and/or Drapes
	Swf(b)	Wavy Laminated Sandstone with Mud Flasers and/or Drapes, Partly Bioturbated
	Sxl(p)	Planar Crossbedded Sandstone
	Sxl(p, hb)	Planar to Herringbone Cross-Laminated Sandstone
Shale	Mmc	Compacted Massive Mudstone
	Ml	Laminated Mudstone
	Mb	Bioturbated Massive Mudstone
Sandstone/ Mudstone Heterolithics	HS	Sand-Dominated Mudstone/Sandstone Heterolithics
	HSw	Wavy-Laminated, Sand-Dominated Sandstone/Mudstone Heterolithics
	HMw(b)	Wavy-Laminated, Mud-Dominated Sandstone/Mudstone Heterolithics, Partly Bioturbated
	HM	Mud-dominated heterolithics

The siliciclastic rocks are differentiated into three main lithofacies types as follows:

Facies A: It is generally composed of sandstone mostly of fine sand, massive - thinly laminated, rippled partly cross laminated and/or bioturbated and occasionally of fining upward nature. Scour and channel features occur in which rip-up mud clasts and chips are included. It is characterized by suitable porosity and permeability properties with oil saturations in the slightly cemented intervals. Two types could be distinguished as A1 and A2 according to the predominant sedimentary structures.

Facies B: This is made up of interbeds of sandstone and shale with small scale migrated ripples, slightly bioturbated with nodular pyritized mudstone concretions.

Facies C: Consists of shale with mudstone, of shallow marine to lagoonal environment, fossiliferous, glauconitic with

Please cite this article in press as: H. Salama et al., Identify re-development concepts to enhance Abu Roash "C" oil reservoir productivity Sitra Area, Abu Gharadig Basin, Western Desert, Egypt, Egypt. J. Petrol. (2016), http://dx.doi.org/10.1016/j.ejpe.2016.04.003

Table 7 Petrographic, SEM & XRD studies, Sitra 8-17 for Abu Roash "C" Member.

Depth m	Lithology (see Table 8, Fig. b)	Thin section (see Table 10, plate 5.3 & 5.5)	Minerals present (see Table 8, Fig. b)	Clay fraction	SEM (see Table 9, plate 6.4 & 6.5)
2848.4	Off-white sandstone, fine grained, positive acid reaction	(2848.3) Silty fine grained Sandstone	Quartz = 94%, Calcite = 2%, Kaolinite = 4%	100% Kaolinite	Quartz grains, mostly corroded, set in clay matrix with few pyrites. Open unconnected micropores
2849.5	Light gray to creamy sandstone, fine grained, muddy, calcareous, poor visual porosity	(2849.2) Degraded glauconitic micritic Sandstone	Quartz = 59%, Albite = 5%, Kaolinite = 10%, Calcite = 25%, Illite = 1%	90% Kaolinite 10% Chlorite	Fine grained quartz & feldspar set in a clayey matrix. Generally poor porosity and local good porosity
2856.2	Light yellow compact fine grained sandstone, non-calcareous	(2855.5) Fine grained Sandstone	Quartz = 70%, Albite = 8%, Kaolinite = 20%, Illite = 2%	100% Kaolinite Tr Chlorite	Rounded & corroded quartz grains set in clay with unconnected micropores. Pyrite framboids
2859	Fine grained, friable sandstone, non-calcareous, good visual porosity. Similar to 2864 m depth sample but friable	(2859.5) Fine grained Sandstone, stylolitic	Quartz = 90%, Albite = 6%, Kaolinite = 4%	100% Kaolinite	Quartz with silica overgrowths and some corroded, with open connected micropores. Good porosity
2860.5	Fine grained, friable sandstone, non-calcareous, good visual porosity. Similar to 2864 m depth sample	(2860.8) Feldspathic Sandstone, glauconitic	Quartz = 91%, Albite = 5%, Kaolinite = 4%	100% Kaolinite	Quartz with silica overgrowths & some corroded. With sealed grain boundaries. Good open micropores
2864	Yellow sandstone, fine grained quartz grains and few opaques, non-calcareous, coaly partitions	Not available	Quartz = 92%, Albite = 3%, Kaolinite = 5%	100% Kaolinite	Quartz grains with silica overgrowths. Open micropores, some are filled with well-developed kaolinite books

nodular and concretionary iron minerals (pyrite and/or siderite). It has parallel, thin laminations and is occasionally massive. (Table 10, plate 33-1).

Facies D: Carbonate facies at the base of the siliciclastic succession represents the shallow marginal marine, possibly the oolitic shoals. It represents a small scale fining and thinning upward character toward the overlying shales of Facies "C". These are carbonate type (may be of the Abu Roash D member) and not related to Abu Roash "C" member.

The Coal is, almost of marsh facies, partly fissile, pyritic with preserved plant tissues.

4.5.1.2. Cyclicity pattern. The main cyclicity pattern of the examined cores and their vertical facies development are presented. The siliciclastic facies demonstrates the dominance of sandstone sequence of different environments varying from tidal channel to washover of tidal complex. The sandstone Facies A, show well defined truncation and scouring features with the underlying shales of Facies C. the lithofacies analysis could distinguish three main sedimentary cycles of which the middle one includes the Oil-bearing sandstone reservoir. The depositional cycles are arranged from base to top as follows:

Cycle 1: (2965.95–2977 m) (Table 11, plate 27)

It is composed of Facies C together with minor occurrence of Facies A and B. Oolitic fossiliferous carbonate facies are developed at the lower part of the cycle that could reflect a deeper environment during the shoaling conditions (may be related to Abu Roash "D"). Molluscan shell remains and bioturbations with common modular forms are the main biogenic and physical features. The shales are almost phosphatic, partly glauconitic and show thin lamination structures. This major cycle includes several minor cycles which generally exhibit the fining upward nature of the sediments. The shale facies dominates the other lithologies exceeding 85% of the total content. The shales represent a shallow subtidal lagoonal facies that overlies the oolitic shoals belts during the lowering of the sea level. Two sub-cycles could be distinguished.

Cycle 2: (2951.35–2965.95 m) (Table 11, plate 23)

The cycle represents a more or less complete sequence of fining upward facies types A, B, C, and D. The lower sandstones represent the incision event of the tidal channels. Two main types of Facies "A" are distinguished according to the predominant sedimentary structures as follow:

Facies "A1" 2959.6–2965.95 m

Massive oil bearing sandstone, thin laminated with occasional carbonaceous detritus and very thin coal streaks of millimetric scale. Rip-Up mud lithoclasts are present at the base of the channel. Faint trough cross-bedding and migrating ripples are occasionally present. The fine sand grade is the dominant grain size. Two truncation surfaces are seen in the upper part.

Facies "A2" 2954.9–2959.6 m

Ripped sandstone with common migrating ripples are recorded at the lower part together with wavy and thin laminations of silty shale streaks (< 10 cm thick each). The upper boundary is characterized by complicated truncations. Reactivation surfaces are also seen denoting the alteration of the dominant tidal (constructional) phase and subordinate (destruction) phase. Weak oil shows are recorded in these sandstones.

Facies "B" and "C"

These are represented at the upper part of the second cycle where sandstone/shale and shale facies are successively developed. They represent the lowering phase of the sea level

Table 8 X-ray Diffraction Analysis (XRD).

Well name	Slide	Description
Sitra 8-1 ST2	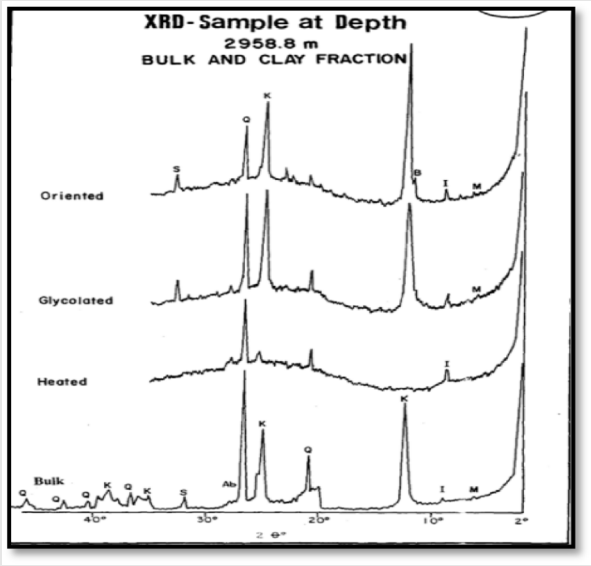	Fig. a Depth 2958.8 m Main constituents: Quartz and clay minerals (kaolinite with minor illite and Montmorillonite) Minor constituents: Siderite and Plagioclase
Sitra 8-17	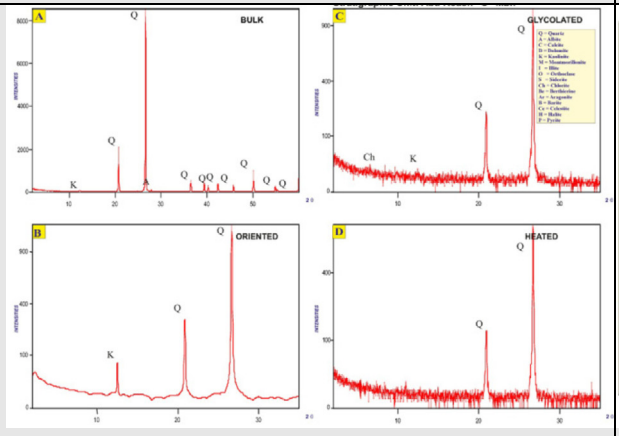	Fig. b Depth: 2859m Fine grained, friable sandstone, non-calcareous, Good visual porosity. Quartz = 90%, Albite = 6%, Kaolinite = 4%

where low tidal sand flat is followed by the high tidal flat muddy facies. The complete restriction leads to the development of coastal marshes where a thin coal seam of peat category was developed (Facies D), to terminate the second cycle.

Cycle 3: (2940.5–2951.35 m) (Table 11, plate 10)

The lower part of this cycle represents an event of rapid rise of fluctuating sea level to develop the non fossiliferous sandstone and shale sequence of Facies B. This was followed by a highly fossiliferous, bioturbated sandstone from 2943.7 to 2947.4 m of Facies A, which reflects a low tidal domain of either strand beach or washover fan facies. Minor sandy mudstone interbeds of Facies C were developed with common shell fragments and bioturbations that denote the possible lowering phase of sea level near the end of this cycle and the dominance of tidal mud flat facies.

Notice: Facies classification in Table 5 and Facies scheme Fig. 15.

4.5.1.3. Sitra 8-1 ST2 petrographic analysis.

- The sandstone petrography indicates the dominance of quartzarenite facies with slight carbonate cement, essentially in the oil bearing zone. The differential dissolution of cement enhanced the development of open and connected intergranular pores (Plate 58-a&b); the process might be due to the action of the acidic connate water accompanied by oil migration.
- Green glauconitic sandstone is dominated in the mudstone (Facies B) of Cycle 1 with subordinates of phosphatic pellets, clasts and minor shell fragments.

Table 9 Scanning electron microscope analysis (SEM).

Well name	Plate number		Slide	Description
Sitra 8-1 ST2	58	a	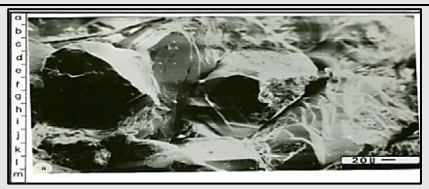	Fig. a Multistage zones of silica overgrowths on quartz grains ensured with minor kaolinite, pores are left opened (depth 2961.1')
		b	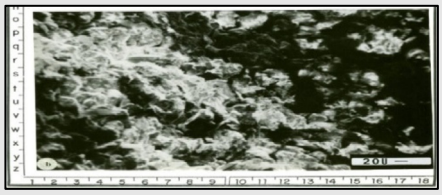	Fig. b Geometry of equisized pores in the oil stained, well sorted sandstone (black areas) depth 2961.1
Sitra 8-17	6.5	b	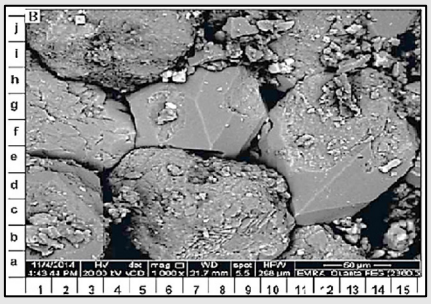	Depth 2860 Open micropores between quartz grains, with silica overgrowth (c-11) & corroded quartz grains (e-14)
	6.4	c	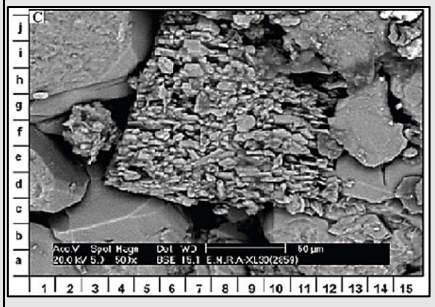	Depth 2859 m Lithic fragment(f.8) with planar texture associating quartz grains, some with silica overgrowth (c-4) with open micro-pores (g-4)

- The XRD analysis of the clay mineral fractions revealed the dominance of a kaolinite and montmorillonite in the shales of the lower cycle with an apparent increase of glauconite mineral in the middle part. The middle cycle that includes the potential sandstone reservoir is characterized by the dominance of kaolinite with subordinate illite in its clay mudstone fractions (Table 8). The upper sedimentary cycle is characterized by kaolinite and illite mineral association with subordinate montmorillonite (about 2%). In the component clay fraction, brushite appears as a monoclinic mineral having the formula $CaH(PO4)_2{\cdot}H_2O$. This mineral is widespread in small amounts in continental phosphate deposits.(Table 8, fig. a).
- The significant fillings are siderite, pyrite and kaolinite.
- The intergranular pores in the oil bearing sandstone are partially filled with laminated kaolinite which permits a certain degree of pore connectivity. (Table 9, plate 58-a&b).
- The silica overgrowths are developed in multistage that show a well-defined zoned pattern.

Table 10 Thin Section Analysis).

Well name	Plate number		Slide	description
Sit 8-1 ST2	33	1	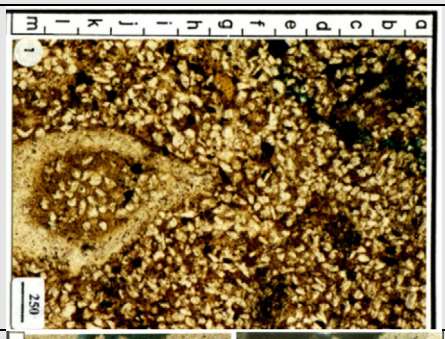	depth 2940.85 m (Facies C) Fossiliferous Quartzwacke Mulluscan shell fragment are partially replaced by silica Partly open-packed texture
	44	3 &4	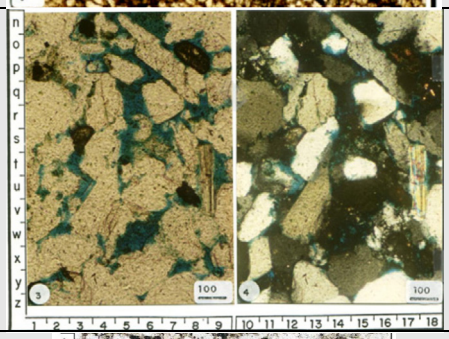	Depth 2959.5 m (Facies A) Quartzarenite (Oil bearing) Fine grained S.S, good porosity due to intergranular connected pores (blue areas) are preserved opened Calcite spars partly blocked the pores
Sitra 8-17	5.3	A&B	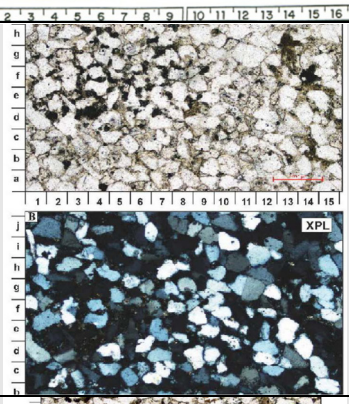	Depth 2855.5 Fine to medium grained sandstone Moderate to well sorted, consists of quartz, opaques (d-2)with clay and clayey-carbonate matrix-cement
	5.5	A&B	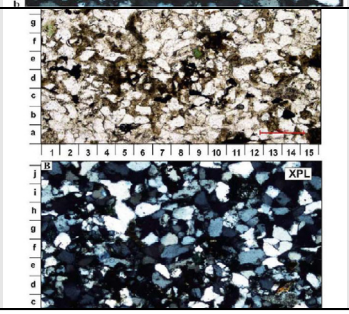	Depth: 2860.8 m Glauconitic feldspathic, fine to medium grained sandstone Immature Set in clayey matrix

➢ The fine grained sandstones are well sorted and have equal pore spacing (Table 10, plate 44-1,2).
➢ The palynologic analysis yielded a rich insoluble organic residue with a poor palynomorph content and high frequency of terrestrial plant tissues. Three palynofacies associations have been identified as follows from base to top.

A. Shallow marine tidal flat including Cycle No.1 and No.2.
B. Restricted marsh around the coal marker at the top of Cycle No.2.
C. Lacustrine to lagoonal restricted domain covering cycle No.3.

Please cite this article in press as: H. Salama et al., Identify re-development concepts to enhance Abu Roash "C" oil reservoir productivity Sitra Area, Abu Gharadig Basin, Western Desert, Egypt, Egypt. J. Petrol. (2016), http://dx.doi.org/10.1016/j.ejpe.2016.04.003

Table 11 Core analysis.

Well name	Plate number		Slide	Description
Sitra 8-1 ST2	10	Cycle 3	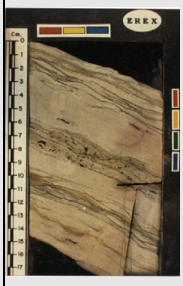	Bottom depth 2949.2 m Sandstone: highly calcareous, showing three fining upward small cycles, each of which is massive at the lower two thirds and rippled, shaly in the upper this of the cycle. Notice the increase of coal detritus in the upper part of the middle cycle.
	23	Cycle 2	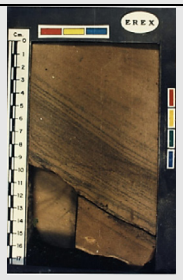	Bottom depth 2959.5m Sandstone, (fl), oil saturated, indurated, thin laminated, slightly Argillaceous, laminae increase in thickness upwards, slightly calcareous, with carbonaceous plant detritus are common downward
	27	Cycle 1	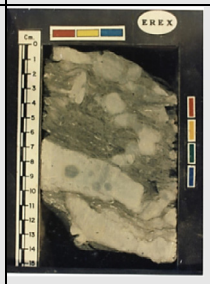	Bottom depth 2967.75 m Fossiliferous, glauconitic, with nodular calcareous mudstone intercalations parallel to the bedding. Some of these modules show vertical position due to pushing up against loading (upper left corner)
Sitra 8-17	4.2	Cycle 3 (MSF)	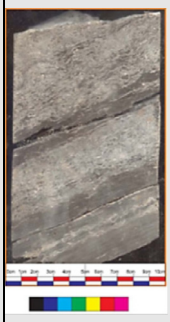	Depth 2840.14-2840.31 m Shale: hard , compact, highly bioturbated, showing alternating lighter (more silty) and darker (more clayey) intercalations, with pelagic bivalve shell
	4.7	Cycle 2 (Reservoir)		Depth: 2863.83-2864.0 m Sandstone Fine grained, brecciated by a network of cracks. A pyritized concretion exists in the upper right part of the slab Lithofacies classification: Sx

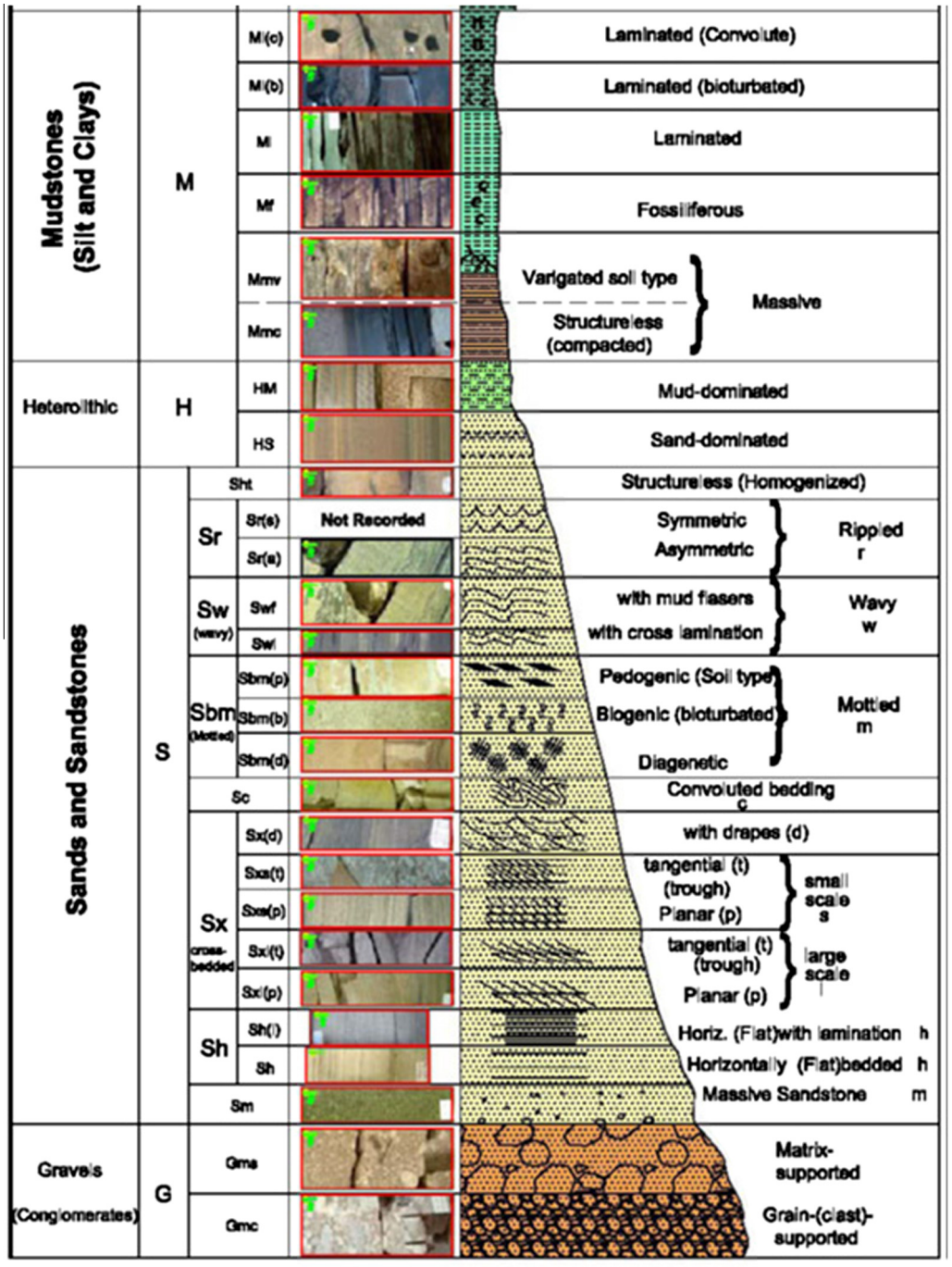

Figure 16 Standard Lithofacies scheme for Siliclastic Sequences.

The Foraminiferal examination could indicate the *Ammomarginulina ovoidea* zone of Turonian age at 2967.5–2977 m, in core No. 2.

4.5.2. Sitra 8-17 ARC cored interval:[17,18]

The same cyclicity pattern for Sitra 8-1B well could be also concluded from Sitra 8-17 core description but with difference in facies distribution.

a. Description

Interval: 2837.40–2864.46 mbdf.

Age: The Interval from 2838 to 2852.5 m is dated as Late Cretaceous (Turonian) and suggesting Abu Roach "C" based on the occurrence of the Small *Ephedripites* < 30 μm and Foraminifera *Discorbis* spp. & *Arenaceous forams*.

Interpreted Genetic Units:

- Sandy and Muddy Tidal Flats (Cycle 3).
- Tidal channel (Cycle 3).
- Swamp (Cycle 2).
- Distributary Mouth bars (Cycle 2).
- Bay Muds (Cycle 1).

Lithofacies Expected Geometry:

Tidal flats: sheet-like parallel to paleo-shoreline.

Channel/mouth bar complex: bars normal to paleo-shoreline.

deposition within shallow water condition subjected to considerable clastic influx terrestrial source.

b. Lithologic description

Interval	Lithology	Lithofacies designation	Description
2837.2 – 2848.1m	Shale	Ml, Mb	Hard, compact, flat laminated, commonly bioturbated, with pelagic pelecypods at the upper levels, with localized calcareous veinlets, and occasional pebble-size calcareous concretions and clasts, locally silty or very fine sand sized showing planar cross lamination, locally rippled, variably calcareous
2848.1–2848.65 m	Sandstone	Sx(p), Sb	Medium-grained, flat to cross-laminated, burrowed, non-calcareous, with pistachio green fluorescence
2848.65–2849.0 m	Sandstone	Sm, Sb, Mmc	Medium-grained, massive, burrowed, interbedded with Shale: thinly laminated, with occasional sandstone lithoclasts and sideritic bands at the bottom
2849.0–2851.1 m	Sandstone	Shl, Swf, Sxl	Fine to medium-grained, wavy to flat laminated partly cross-bedded, with occasional mud drapes and flasers, lithoclasts and ferruginated laminae, variably calcareous, highly oil-stained at the middle part
2851.1–2851.60 m	Shale	Mmc, Shl, HSw	Blocky to sub-blocky, non-calcareous, intercalated with fine to medium grained flat-laminated Sandstone, and wavy laminated sand-dominated Heterolithics
2851.6–2852.1 m	Coal:	C	Medium hard to brittle, massive to slightly laminated
2852.1–2853.8 m	Shale	Mmc	Blocky to sub-blocky, non-calcareous with occasional ferruginated concretions and lithoclasts
2853.8–2854.96 m	Sandstone	Swf(b), Mmc, HMw(b)	Fine to medium-grained, wavy-laminated with mud drapes and flasers, with occasional burrows and ferruginated concretions, intercalated with blocky to sub-blocky non-calcareous Shale and mud-dominated, wavy-laminated occasionally burrowed Heterolithics bottomed by pebble-size sandstone clasts
2854.96–2864.20 m	Sandstone	Shl, Sx(p, hb), Swf	Fine to medium-grained, flat to cross-stratified, locally herring-bone cross-laminated, wavy flasers and mud-drapes are presents at some intervals, with scattered dark colored lithoclasts near the top, and burrows and cracks at the base, non-calcareous. The sandstone shows coarsening upward grain-size pattern

Biostratigraphic analysis

Foraminiferal analysis

Interval (m)	Biozone	Age	Rock unit
2838 m–2852 m	*Discorbis* spp. & *Arenaceous forams*	Middle Turonian	Possible Abu Roash (C)
3244.6 m–3253.4 m	Barren	Undetermined	Undefined

Palynological analysis:

Core samples 2851.31 & 2852.5: Turonian

Marker species: Small *Ephedripites* < 30 μm.

Assemblage: *Tricolpites* sp., *Liliacidites* sp., *Inaperturopollenites* sp., *Cyathidites minor*, *Gabonisporites* sp., and *Cycadopites* sp.

Age: Turonian

Paleoenvironment interpretation:

It is a rich yellow brown phytoclasts with high percentage of amorphous organic matter (AOM). The palynofloras recorded from this sample are dominated by terrestrial sourced miospores. This type of palynofacies, beside the common occurrence of fresh water algae (Pediastrum algae) reflects

c. Interpretation of the lithofacies analysis and depositional environment (Table 6) and Fig. 16.

d. Sitra 8-17 Petrographic, SEM and XRD Analysis Table 7.

e. Depositional Environment Interpretation from the Well Sitra 8-17.

The depositional setting of the studied intervals is an example of the tide-dominated estuaries, where Abu Roash "C" Member was deposited in two depositional settings; the first one is the tidal dominated environment from the northern direction includes Tidal channel, tidal bar and tidal flat sands and are associated with brackish water mudstone, tidal flat mudstone, coal fragments and coaly shale. This is clearly identified from the log character of the Sitra 8-1 ST2 well.

The second depositional setting is the fluvial deposits represented by the distributary mouth bars (Coarsening upward pattern) coming from the south, and it is clearly identified from the log character of the Sitra 8-17 well (Fig. 17).

The identified lithofacies types could be grouped into a number of closely related lithofacies associations indicative of corresponding genetic units, namely:

Please cite this article in press as: H. Salama et al., Identify re-development concepts to enhance Abu Roash "C" oil reservoir productivity Sitra Area, Abu Gharadig Basin, Western Desert, Egypt, Egypt. J. Petrol. (2016), http://dx.doi.org/10.1016/j.ejpe.2016.04.003

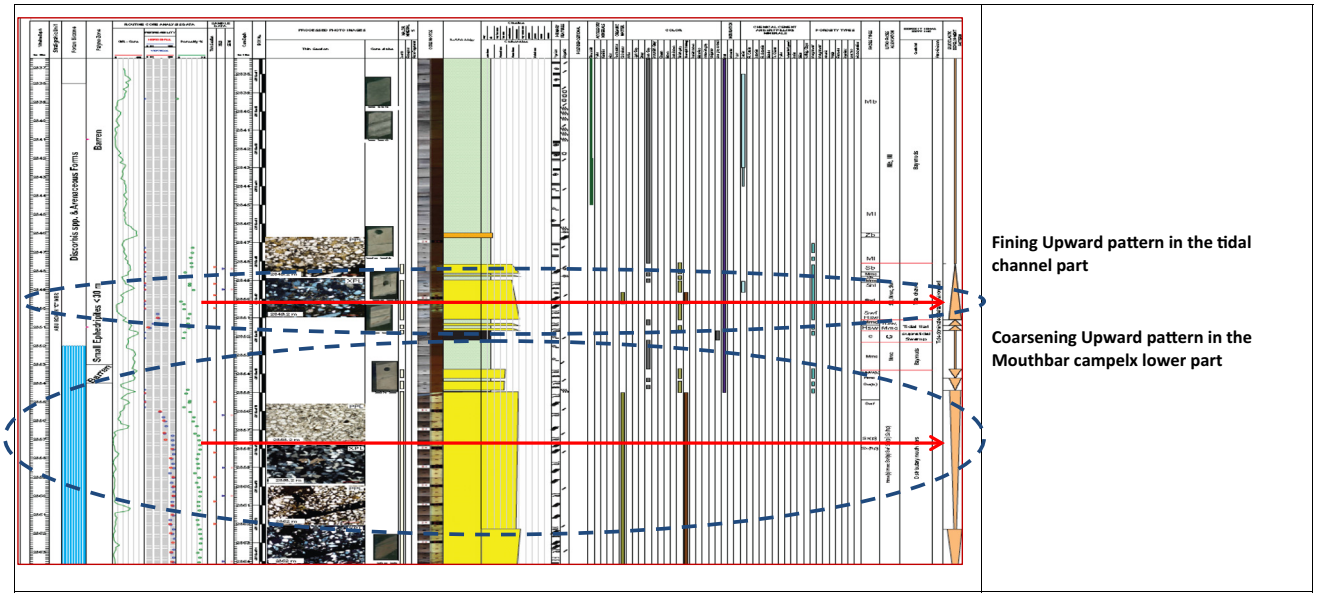

Figure 17 The Core Log for Sitra 8-17 well showing different diagenetic units and facies distribution.

- Sandy and Muddy Tidal Flats
- Swamp
- Tidal channel
- Distributary Mouth bars
- Bay Muds

From the Routine Core analyses of this well we found a great difference in reservoir behavior and the petrophysical parameters of the 2 parts of this reservoir (the tidal channel and the mouthbars).

Tidal channel sandstone	Interval: 2849.13–2851.08 m	Average H. Permeability = 1.6 mD Average V. Permeability = 1.36 mD Helium Porosity = 9.4%
Mouth bars sandstone	Interval: 2855.02–2864.03 m	Average H. Permeability = 383.91 mD Average V. Permeability = 265.7 mD Helium Porosity = 21.8%

4.6. Analyses results

4.6.1. X-ray Diffraction Analysis (XRD) (Table 8)
4.6.2. Scanning Electron Microscope Analysis (SEM) (Table 9)
4.6.3. Thin Section Analysis (Table 10)
4.6.4. Core Analysis (Table 11)

5. Discussion

From All detailed analysis (lithological, sedimentological, and Petrophysical) especially after combination of Sitra 8-1 ST2 cored data with the other cored intervals of Abu Roash "C" from the well Sitra 8-17 we can conclude the following about ARC member:

Age: Late Cretaceous (Turonian time)

From the Interpretation of AR"C" member Genetic Units:

3 depositional cycles differ from each other in Facies classification, distribution and reservoir characterization.

In Sitra Area: two major parasequences were identified, the first lower one was developed during a shallowing upward sequence represented by shale/ sand intercalations into which the main Abu Roash "C" reservoir sand bodies are included, and reached its end by the appearance of a laterally extended coal marker nearly one meter thick. This parasequence was deposited subsequently to a falling sea level phase which occurred after the deposition of Abu Roash "D" limestone. The succeeding parasequence (deepening upward) reached its maximum flooding surface (MFS) by the deposition of the widely extensive shale marker being rich in pelagic Pelecypod shells.

The resultant stratigraphic units consist of: genetically related depositional cycles (3 cycles) and their components of facies sequences (5 facies types), each cycle has its own distribution, facies classification and reservoir characteristics. (Fig. 18 for Line of Section (1) and Fig. 19 for Line of Section (2)).

As mentioned in the published literature "tidal depositional systems remain the least well understood compared with their fluvial-dominated and wave-dominated counterparts. As a consequence, facies models for tidal depositional systems have remained more uncertain, partly because of the difficulty of separating local variability from the broader generic aspects (e.g. [34]). Even where a tidal depositional setting is interpreted with confidence from facies-scale observations, often it is not clear whether, for example, the deposits were part of a transgressive estuarine depositional system or, instead, part of a regressive, tide-dominated delta system". Both areas accumulate similar facies but the larger scale architectural styles and

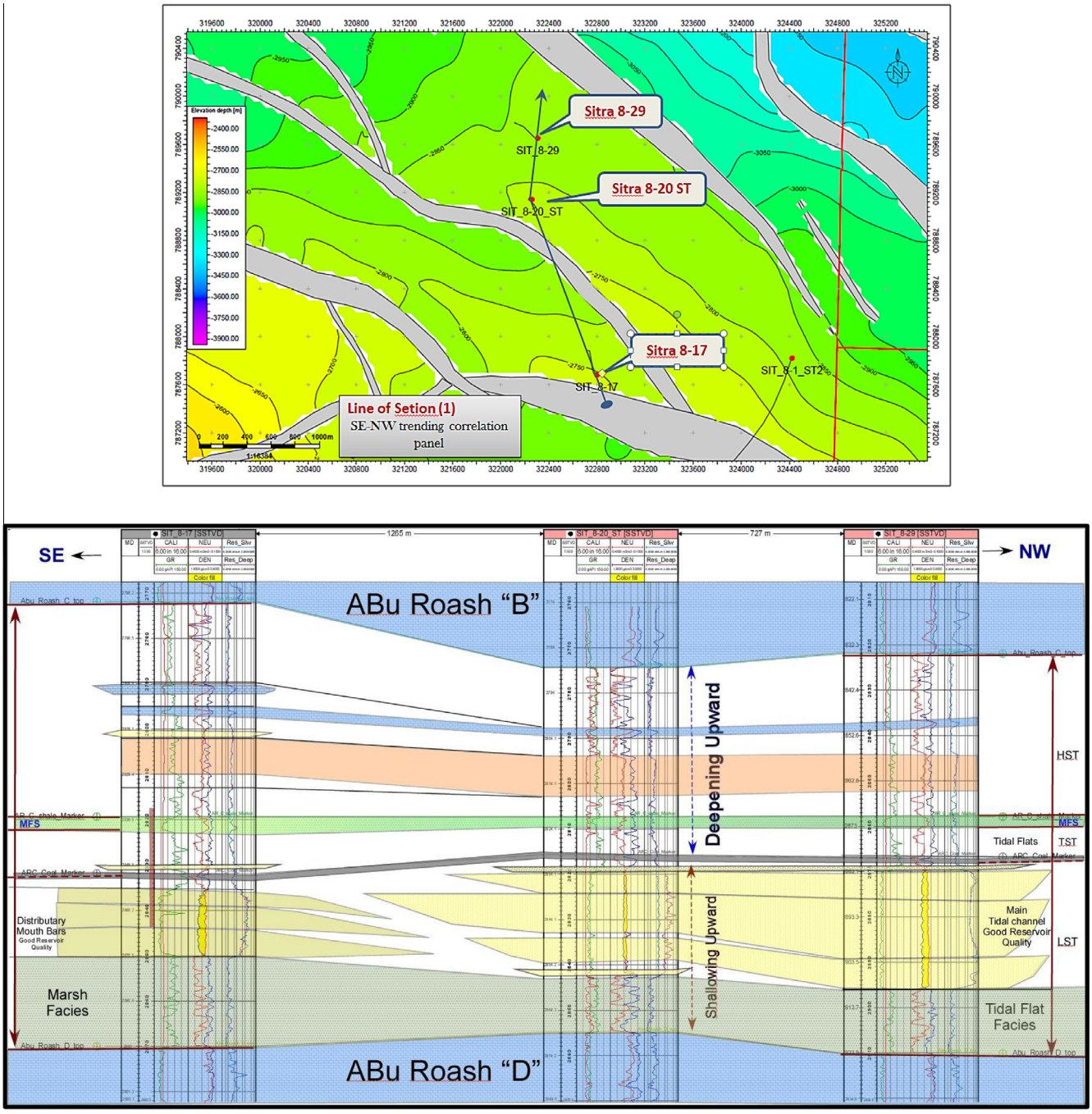

Figure 18 SE–NW Correlation panel (Line of Section 1) representing the depositional environment and facies change of Abu Roash "C" deposited during the Turonian Time. (the main tidal channel path from the NW direction clearly represented in Wells Sitra 8-29 and ended somewhere after Sita 8-20 ST to meet the path of the Fluvial source coming from the SE direction clearly represented by the mouth bars in the Sitra 8-17 well).

facies trends are different. And before jumping to a conclusion for the AR"C" depositional environment lets show the following illustrations (Fig. 20) [68].

[52], defined an estuarine sequence as "a complex of intertidal and shallow subtidal, mostly channel-form intracoastal facies dominated to some extent by tidal processes exhibiting conspicuous variations in sediment texture, composition, and provenance, and in physical and biogenic sedimentary structures". The depositional environments comprising this complex of facies may encompass any number (or all) of the following: tidal channels, tidal deltas, inlets, shoals, back-barrier beaches and spits, washover fans, swash and point bars, tidal flats, marshes, and stream banks [106].

After the detailed results and discussion, we can easily identify two different depositional settings in our study area which resulted from calibration of all data with the logging analyses.

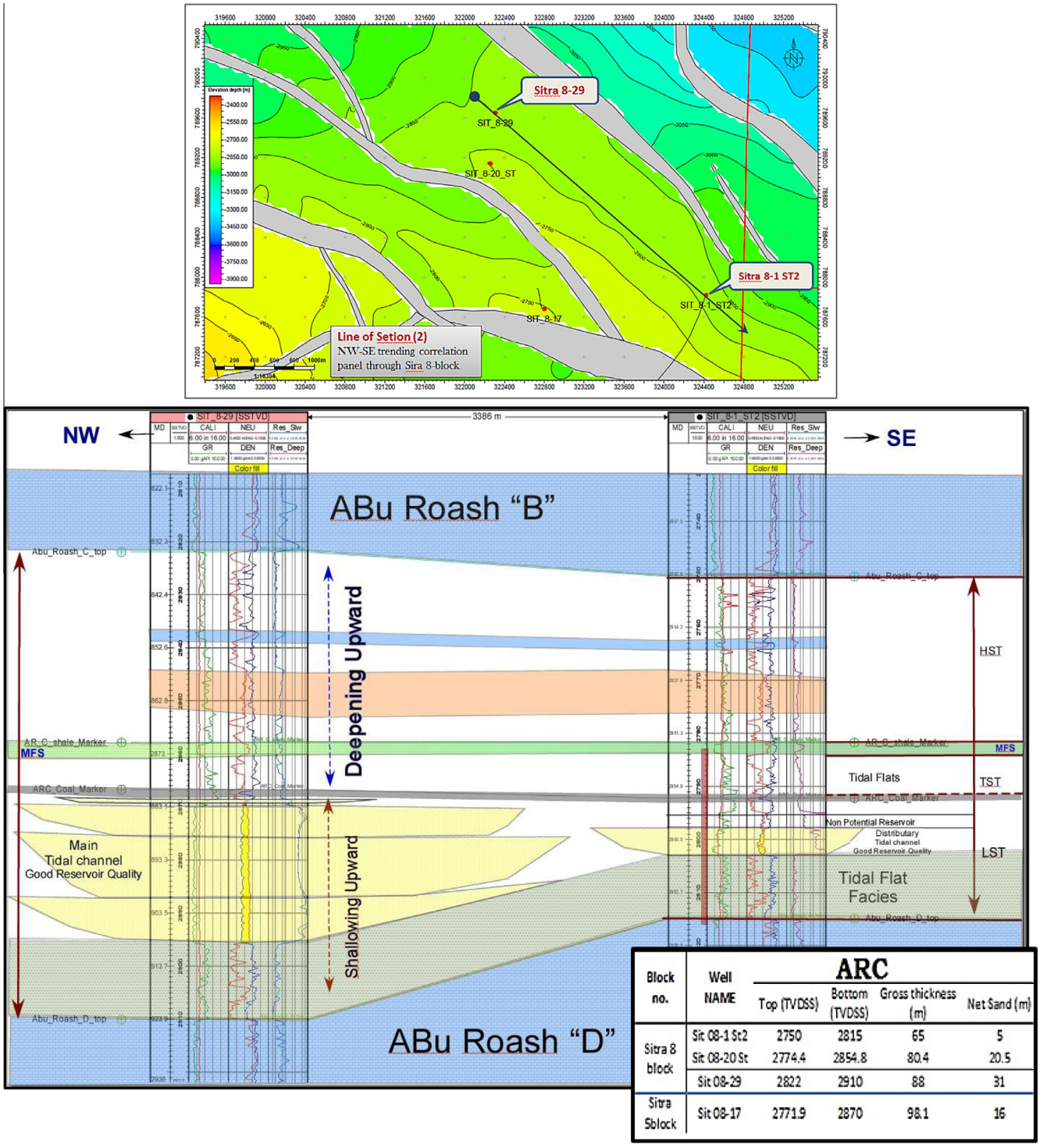

Block no.	Well NAME	ARC Top (TVDSS)	Bottom (TVDSS)	Gross thickness (m)	Net Sand (m)
Sitra 8 block	Sit 08-1 St2	2750	2815	65	5
	Sit 08-20 St	2774.4	2854.8	80.4	20.5
	Sit 08-29	2822	2910	88	31
Sitra 5block	Sit 08-17	2771.9	2870	98.1	16

Figure 19 NW–SE Correlation panel(Line of Section 2) (representing the main tidal channel in Sitra 8-29 well with the maximum thickness of 30 m sand and a distributary tidal channel in sitra 8-1 ST2 emerged from the main channel as shown in this correlation panel).

The Abu Roash "C" member exhibits all of the characteristics of the Shallow Marine-Tidal dominated environment which linked to the south with a fluvial system during Turonian time, the tidal dominated system are clearly identified and represented in tidal channels and tidal flat facies, march deposits, and distributary mouth bars. The best reservoir rock in the Abu Roash "C" was deposited as distributary channel fill that cut through the underlying strata (Fig. 21).

Modern Analogs-Tide dominated Estuaries:

Many Analogs around the world could be taken an example for the same depositional settings of Abu Roash

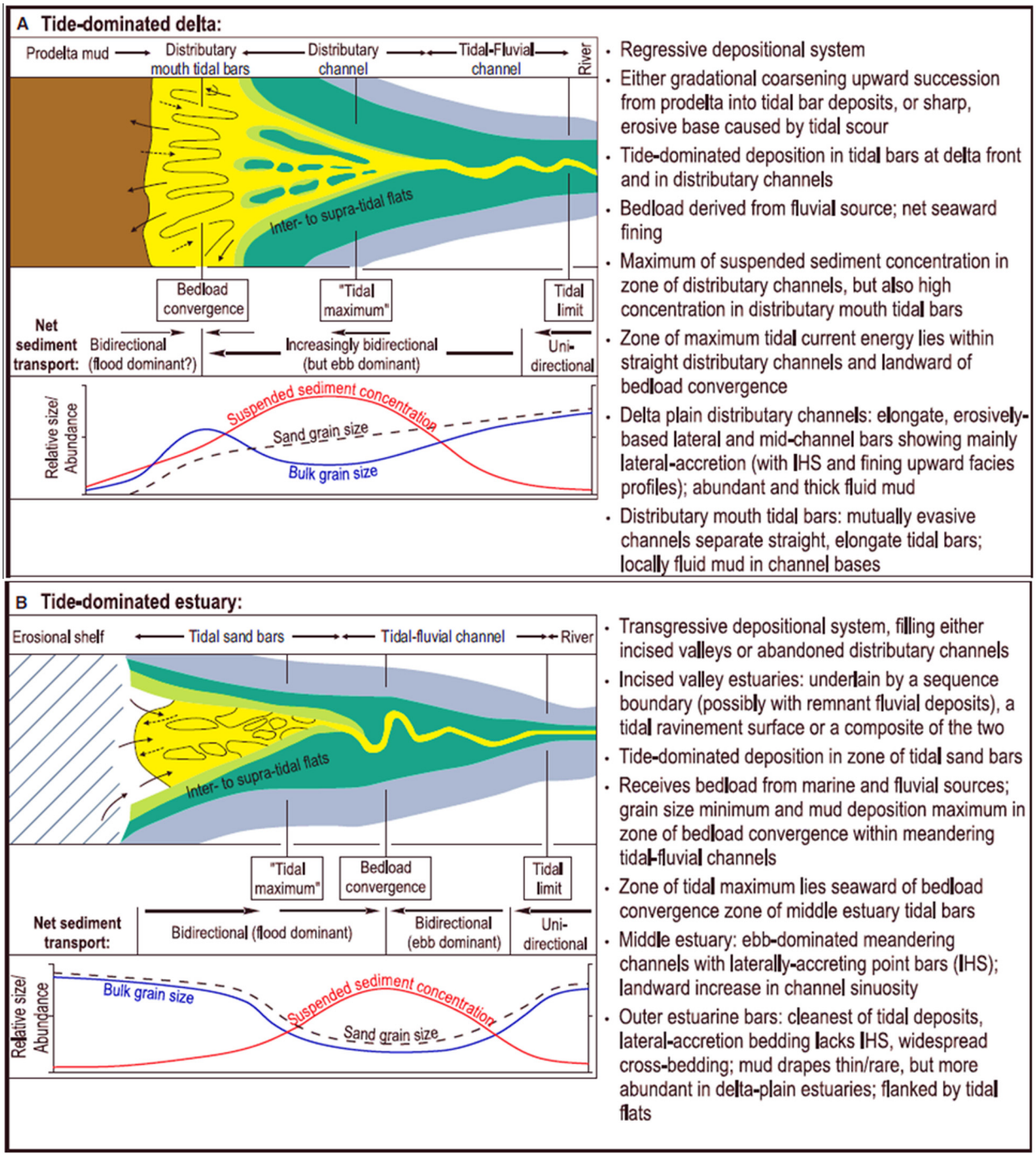

Figure 20 Summary of tide-dominated depositional environments. A generalized map shows sub-environments and the associated net sediment transport directions, and relative grain size of sediments resulting from changes in process energy down-depositional dip. Diagnostic characteristics of each environment are listed. (A) Tide-dominated delta. (B) Tide-dominated estuary (based on Dalrymple & Choi, 2007).

"C" member (i.e. Morondava Coast in Madagascar (Fig. 22) and Pakistan Coast (Fig. 23)).

Production Data (Table 12).

A/R "C" reservoir description

The A/R "C" sand reservoir consisting of tidal channels & sand flats is believed to be latterly extensive in the Sitra 8 area. RDT data acquired in Sitra 1B, 2 and 5 shows that the sands are in pressure communication despite some of these wells are more than 3 km away from each other. The average Net to Gross is high (more than 50%). The porosity range between 9% and 19% and permeability between 20 mD and 1D with best reservoir properties observed in the clean tidal channels

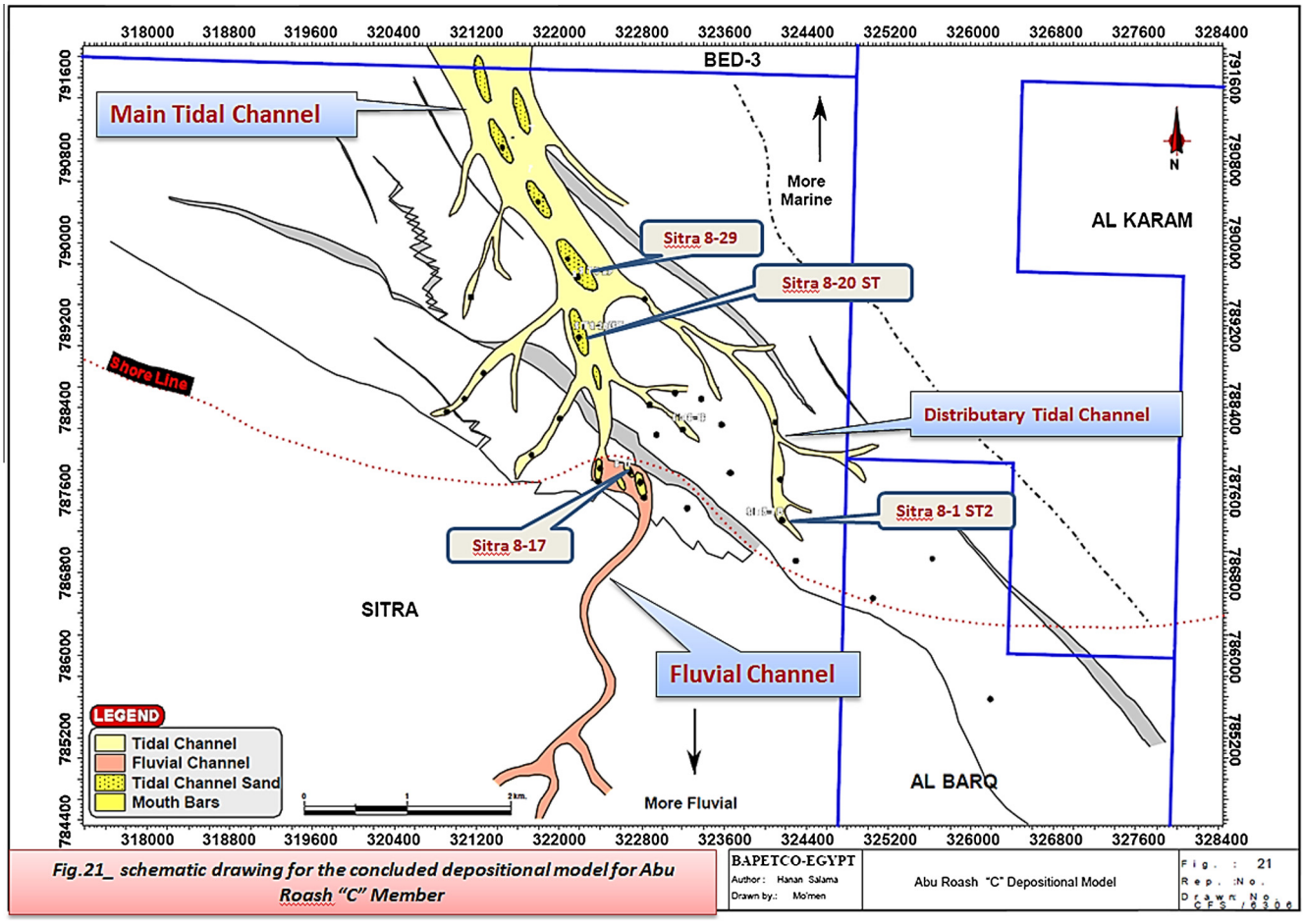

Figure 21 schematic drawing for the concluded depositional model for Abu Roash "C" Member.

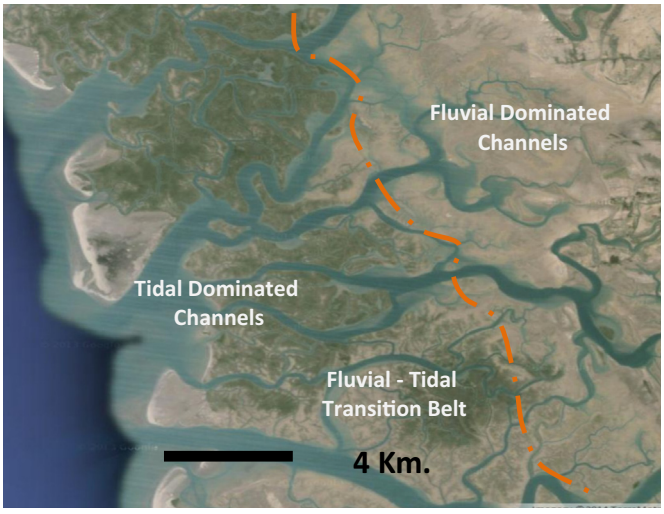

Figure 22 Pakistan Coast.

(K up to 500 mD) with an expected preferential NW-SE orientation (channel orientation). Despite possible local reservoir deterioration can locally occur (mud flats) [22].

From the production data and the illustrated map (Fig. 24).

- We have two structural blocks in Sitra Area where AR"C" exhibit different behaviors as a result we noticed two different ODT.

Please cite this article in press as: H. Salama et al., Identify re-development concepts to enhance Abu Roash "C" oil reservoir productivity Sitra Area, Abu Gharadig Basin, Western Desert, Egypt, Egypt. J. Petrol. (2016), http://dx.doi.org/10.1016/j.ejpe.2016.04.003

Figure 23 Morondava Coast (Madagascar).

Table 12 Production data.

Well name	Well_status for (AR/C)	Perforated intervals	Production performance		Fluid contacts	STOIIP (MMstb)		
			Strat (BOPD)	Now (BOPD)		LC	BC	HC
Sit 08-01 ST2	On Production	2961–2973	4300	163	ODT: 2909	$5^{(8\text{-block})}$	$7.5^{(8\text{-block})}$	$10^{(8\text{-block})}$
Sit 08-20 ST	On Production	2839–2856	942	2400		$10.5^{(8\text{-block})}$	$28^{(8\text{-block})}$	$45^{(8\text{-block})}$
Sit 08-29	Watered Out	2885–2892	629	0				
Sit 08-17	Watered Out (production switched to Bahariya Reservoir)	2856–2870	2500	0	ODT: 2850 WUT: 2898	$5^{(5\text{-block})}$	$7.5^{(5\text{-block})}$	$13.1^{(5\text{-block})}$

LC: which is the ODT (*ODT***Oil Down To*).
HC: which is either the maximum reservoir closure or the WUT (*WUT**Water Up To).
BC: which is the mid-point between the LC & HC.

- A/R "C" member in Sitra 8 area forms an attractive reservoir for water flooding based on the evidence of reservoir connectivity.
- In the Sitra 5 block the A/R "C" reservoir penetrated despite thinner exhibits similar good reservoir quality than in Sitra 8 block.

6. Conclusion

Sitra area is divided into many Structural blocks; the main producing one is the Sitra 8 block in which 39 wells were drilled since 1993 started with the drilling of Sit 8-1 well; till 2015 with the drilling of Sit 8-39 well. Various data form these wells were evaluated to form a detailed depositional facies models for the Abu Roash "C" reservoir, the log analysis was tied to the core descriptions, and ditch cuttings data to provide a relationship between log response, lithology, depositional facies, and reservoir characteristics.

In Sitra Area the Abu Roash "C" is approximately 60–90 m thick and exhibits all of the characteristics of the shallow marine tidal dominated estuaries which is linked to the south with a fluvial system during Turonian time, the tidal dominated system are clearly identified and represented in tidal channels and tidal flat facies, march deposits, and distributary mouth bars. The best reservoir rock in the Abu Roash "C" was deposited as distributary channel fill/Mouth bars that truncate the underlying strata.

According to [53]'s definition for the sequence boundaries, in Sitra Field two major parasequences were identified, the first lower one was developed during a shallowing upward sequence represented by shale/ sand intercalations into which the main Abu Roash "C" reservoir sand bodies are included, and reached its end by the appearance of a laterally extended coal marker nearly one meter thick. This parasequence was deposited subsequently to a falling sea level phase which occurred after the deposition of Abu Roash "D" limestone. The succeeding parasequence (deepening upward) reached its

Please cite this article in press as: H. Salama et al., Identify re-development concepts to enhance Abu Roash "C" oil reservoir productivity Sitra Area, Abu Gharadig Basin, Western Desert, Egypt, Egypt. J. Petrol. (2016), http://dx.doi.org/10.1016/j.ejpe.2016.04.003

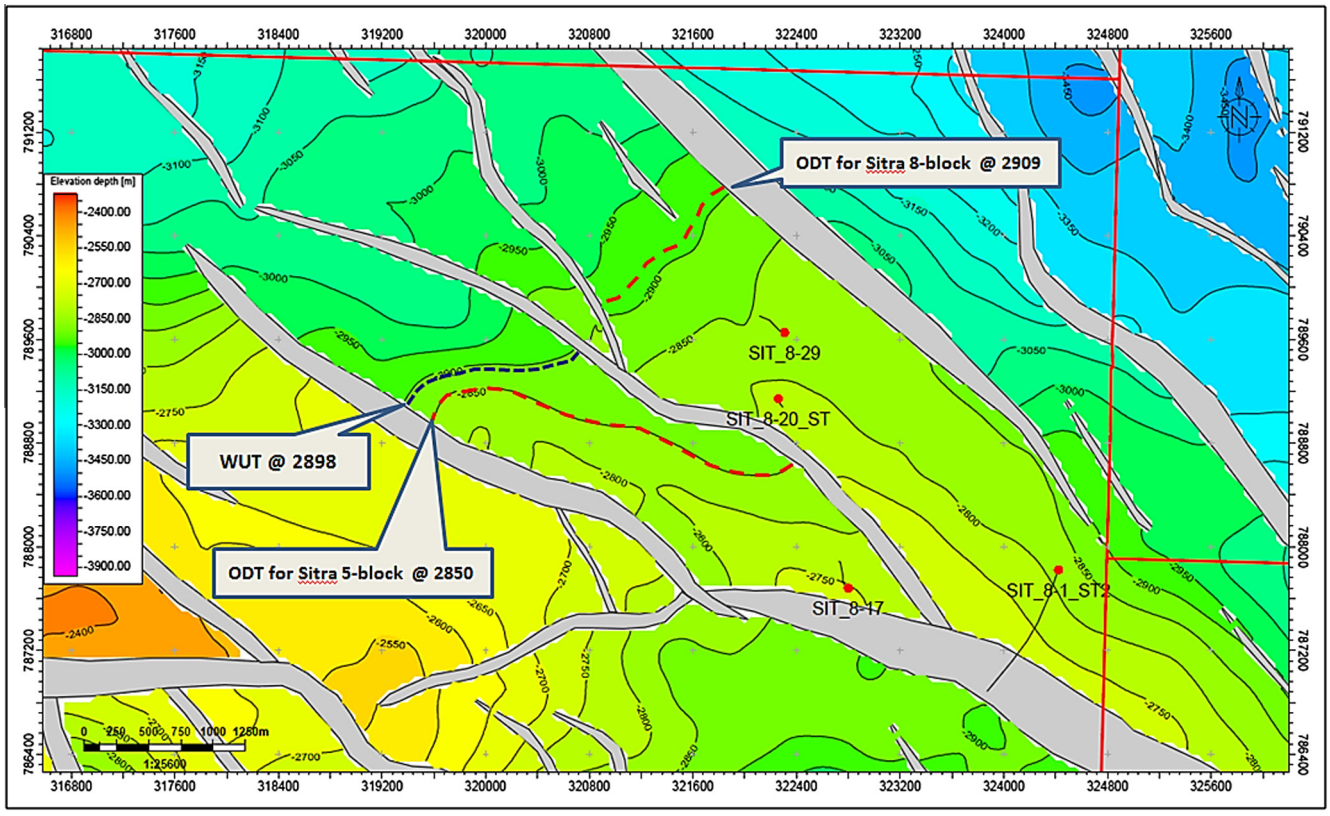

Figure 24 ARC Structural contour map showing the Fluid contacts of both blocks sitra 8 and sitra 5(yellow is more shallow, blue is more deep) (ODT * Oil Down To , WUT * Water Up To).

maximum flooding surface (MFS) by the deposition of the widely extensive shale marker being rich in pelagic Pelecypod shells. The upper part of AR"C" Member represents the high stand systems tracts (HST) of this sequence and consists of silt, shale and some limestone interbeds.

The resultant stratigraphic units consist of: genetically related depositional cycles (3 cycles) and their components of facies sequences (5 facies types), each cycle has its own distribution, facies classification and reservoir characteristics.

The new understanding of the depositional model for ARC Member as a part of the Paralic environment, [47] reveals the major affecting factors that controls the behavior of this reservoir through time and consequently offers a great opportunity for the field's future development activities through a new philosophy to maximize the field ultimate recovery and generate a development plan for Sitra Area that identify the benefits from drilling new development/appraisal wells and applying water injection projects.

This study didn't catch the upper part of AR"C" Member in details due to the very poor quality of the thin sand streaks deposited and hence its low potentiality.

7. Recommendations

- The new depositional model and facies classification of this study recommend further appraisal activities in the southern part of sitra 8 and 5 blocks to confirm and detect the actual path and distribution of the southern fluvial (channel/channels) for more hydrocarbon productivity.
- The A/R "C" Member in Sitra 8 area forms an attractive reservoir for water flooding based on the evidence of reservoir connectivity.
- The A/R "C" Member in the northern part of Sitra 8 block is watered out (only could be used for water flooding).
- The water injection in AR"C" member is very useful in the southern part of Sitra 8 block as discussed in the production data of the Sitra 8-20 St Well.

Acknowledgement

I am grateful to the Egyptian General Petroleum Corporation (EGPC) for their acceptance on the data and to give me this opportunity to finish this study.
I'm thankful to BAPETCO Management for supporting me and giving me the opportunity to work on the data and to complete this study.
A special gratitude should be offered to MR. Mohammed El-Tonbary (Bapetco deputy Exploration Manager & Shell Egypt Regional studies manager) for his valuable comments and reviewing.
My gratitude to my colleague in BAPETCO; geologists and geophysicists, Petroleum Engineering dep., and to Bapetco Drafting department especially Mr. A. Rashwan and Mr. M. Gouda.

A special thanks to Mr. A. El Toukhy from Shell Egypt for teaching me how to work on the PETREL software.

References

[1] Hydrocarbon potential of Abu Gharadig Basin in the Western Desert, Arab Republic of Egypt, in: 8th Arab Petroleum Congress, Algiers, 81 (B-3), 1972.
[2] Jurassic deep project in the Abu Gharadig Basin, North Western Desert of Egypt, in: 12th EGPC Conference, Cairo, Egypt, 1994, pp. 1–20.
[3] Structural framework of the Abu Gharadig Basin, Western Desert, Egypt, in: 9th Petroleum Exploration and production Conference, EGPC, Cairo, 1988, 16 p.
[4] The structural setting and hydrocarbon potential of the Kattaniya Horst and El Gindi Basin, Western Desert, Egypt, in: 10th Petroleum Exploration and production Conference, EGPC, Cairo, 1990, 25 p.
[5] Jurassic source rock maturity and thermal history modeling of the Khalda West Area, North Western Desert, Egypt, in: 12th Petroleum Exploration and production Conference, EGPC, Cairo, II, 1994, pp. 217–233.
[6] Impact of basin inversion on hydrocarbon habitat in the Qarun Concession, Western Desert, Egypt, in: 14th Petroleum Exploration and production Conference, EGPC, Cairo, I, 1998, pp. 139–155.
[7] Evaluation of possible source rocks in Faghur-Siwa Basin, Western Desert, Egypt, in: 10th Petroleum Exploration and production Conference, EGPC, Cairo, I, 1996, pp. 417–432.
[8] Microfloras from the Upper Cretaceous near Aswan, Southern Egypt, Neues Jahrbuch Geologic Palaeontologie Monatshefte, 1991, pp. 711–727.
[9] The effect of thermal burial history in the hydrocarbon maturation and generatin in Central Northern Western Desert of Egypt, Using Subsurface Geophysical and Geological Data; EGS 7th Annual Meeting, 1989, pp. 88–111.
[10] Lower cretaceous Aptian Sediments and There Oil Prospects in the Northern Western Desert, Egypt; 8th Arab Petroleum Congress, Algiers, 74 (B-3), 1972.
[11] Oil and gas discoveries in the Northern Desert of Egypt; Internal Report, Western Desert Operating Petroleum Company (WEPCO), 1974, pp. 1–27.
[12] Paleozoic and Mesozoic depocentres and Hydrocarbon Generating Areas, Northern Western Desert; 7th EGPC Exploration and Production Conference, Cairo, Egypt, 1984, pp. 269–287.
[13] Subsurface Features and Oil Prospects of the Western Desert, Egypt; 3rd Arab Petroleum Congress, Alexandria, 1961, 8 pp.
[14] Geophysical investigation and petroleum geology in the area East of Qattara depression, Egypt (Ph.D. thesis), Faculty of Science, Cairo university, Cairo, Egypt, 1977, 16 p.
[15] Syrian Arc Structures; A unifying Model of Inverted Basins and Hydrocarbon Occurrences in North Egypt, in: 13th EGPC Petroleum Exploration and Production Conference, 1996, pp. 40–60.
[16] Final Well Report Sit 8–1B, 1993.
[17] Conventional core analyses study for Sitra 8–17 well, 2012.
[18] Final Well Report Sit 8–17, 2011.
[19] Final Well Report Sit 8–20 ST, 2012.
[20] Final Well Report Sit 8–29, 2013.
[21] Sitra 8-1B Sedimentological, and Biostratigraphic Studies on Cores No. 1, 2 Parts I and II, 1993.
[22] Sitra Field Development Plan (FDP), 2012.
[23] Wrench Faulting and its implication on Hydrocarbon Accumulations, Alamein-Yidma Area, Western Desert, Egypt, in: 10th EGPC Petroleum Exploration and Production Conference, Vol. 2, 1993, pp. 257–289.
[24] Abu Roash "G" Upper Unit. Environment of deposition and Reservoir distribution; Bapetco Exploration, 1994.
[25] General Review of the Petroliferous Provinces of Egypt with special emphasis on their geologic setting and Oil Potentialities; Energy Project, Petroleum in Western Desert, Egypt (2000), 1982.
[26] The Cretaceous Region of Abu Roash, Near the Pyramids of Giza, Egypt; Survey Department, Cairo, Egypt, 1902, 48 p.
[27] Topography and the Geology of the Faiyum Province of Egypt; Geological Society of Egypt, 1905, 101 p.
[28] Standard Planktonic Zones in Egypt, in: P.H. Bronnimann, H. Renz (eds.), Proc. of the 1st International Conference Planktonic Microfossils, Geneva, 1967, pp. 92–103.
[29] Hydrocarbon Source Rock Evaluation of Upper Cretaceous "Abu Roash Formation", East Abu Gharadig Area, North Western Desert, Egypt; M.E.R.C., Ain Shams University, Earth Science Ser., vol. 1, 1987, pp. 120–150.
[30] Lithofacies and Biofacies of Early Cretaceous in Mersa Matruh Well No. 1, Western Desert, Egypt; Cairo University, 8th Arab Petroleum Congress, 1972, 27 p.
[31] The Influence of Interaction of Depositional Environment and Synsedimentary tectonics on the Development of some Late Cretaceous Source Rocks, Abu Gharadig Basin, Western Desert, Egypt; Egyptian General Petroleum Corporation, Cairo, Egypt, 1996, pp. 475–496.
[32] Synsedimentary Tectonics and Distribution of Turonian Sandstone Reservoirs, Abu Gharadig Basin, Egypt, in: 12th Petroleum Exploration and Production Conference, EGPC, Cairo, I, 1994, pp. 351–367.
[33] Paleozoic Rocks Distribution and Hydrocarbon Potential in the Western Desert, Egypt, in: 11th Petroleum Exploration and Production Conference, EGPC, Cairo, 1992, pp. 56–78.
[34] Morphologic and facies trends through the fluvial–marine transition in tide-dominated depositional systems: a schematic framework for environmental and sequence-stratigraphic interpretation, Ch.4 and 5, 2007.
[35] Geology and Mode of Hydrocarbon Occurrence in the Late Cenomanian – Early Turonian, Abu Sannan Area, Western Desert, Egypt; M.E.R.C., Ain Shams University, Earth Science Ser., vol. 3, 1989, pp. 106–127.
[36] Sedimentology, Environmental Conditions and Hydrocarbon Habitat of the Bahariya Formation, Central Abu Gharadig Basin, Western Desert, Egypt, in: 12th EGPC Petroleum Exploration and Production Conference, 1994, pp. 429–450.
[37] Sequence stratigraphy and Facies of the Jurassic-Lower Cretaceous rift systems in NE Africa, 2008.
[38] Late Cretaceous Tectonics and Starved Basins Conditions, Abu Gharadig Basin in North Western Desert, Egypt, in: 7th Exploration Seminar, EGPC, Cairo, 1984.
[39] The Petroleum potential of Egypt, 2000.
[40] Oil potential of the upper cretaceous sediments in Northern Western Desert, Egypt (M.Sc. thesis), Alexandria Univ., 1991, 165 p.
[41] Basin analysis and hydrocarbon potentiality of Matruh Basin North Western Desert, Egypt, in: 3rd International Conference Arab World (GAW), Cairo Univ., Cairo, 1996, pp. 595–624.
[42] Western Desert, Oil and Gas Fields (A Comprehensive overview), 1992, p. 9–43.
[43] Petroleum geology, in: Said, R. (ed.), The Geology of Egypt, Balkema, Rotterdam, 1990, pp. 567–599.
[44] Cretaceous Rock Units of the Western Desert of Egypt, in: 13th Annual Meeting of the Geologic Society of Egypt, 1975, 2 p.
[45] Structural evaluation of the Eastern Part of the Western Desert and its implications for hydrocarbon, in: 14th Petroleum Exploration and Production Conference, EGPC, Cairo, I, 1998, pp. 156–177.

[46] The structural setting of the Central Western Desert, Egypt, in: 10th EGPC Seminar, Cairo, Egypt, 1990.
[47] Sequence stratigraphy, Chapter 8, 1996, p. 134–153.
[48] Oil and gas discoveries in Western Desert, Egypt (Abu Gharadig and Razzak Fields), in: 4th Petroleum Exploration Seminar, EGPC, Cairo, 1974, pp. 1–16.
[49] Contribution to the stratigraphy of Abu Roash and the History of the Upper Cretaceous in Egypt, Bull. Faculty of Science, Cairo University, 27, 1948, pp. 221–239.
[50] Regional Geological Evolution of the Western Desert, Egypt. 1 St Int. Conf. Geol. of the Arab World, 1992.
[51] Geological Survey of the West Coast of the Gulf of Suez; Report Standard Oil Conference, Egypt, 1942, 52 p.
[52] Mesotidal estuarine sequences: a perspective from the Georgia Bight: Journal of Sedimentary Petrology, vol. 56, 1986, p. 91 1–924.
[53] Genetic stratigraphic sequences in basin analysis: architecture and genesis of flooding surfaces bounded depositional units. AAPG Bull. 73 (1989) 125–142.
[54] The Geochemical Characteristics of Mesozoic and Tertiary Hydrocarbons in the Western Desert and Nile Delta Basins, Egypt, in: 13th Petroleum Exploration and Production Conference, EGPC, Cairo, I, 1996, pp. 401–416.
[55] Organochemical Evaluation of Potential Source Beds and Oils Generation in Abu Gharadig Basin, North Western Desert, Egypt, in: 11th Petroleum Exploration and Production Conference, EGPC, Cairo, 1992, pp. 99–218.
[56] North Western Desert, in: Said, R., (ed.), The Geology of Egypt, Balkema, Rotterdam, 1990, pp. 293–319.
[57] The Jurassic Sediments in Abu Gharadig Basin are Promising Reservoir and Source, in: 12th Petroleum Exploration and Production Conference, EGPC, Cairo, II, 1994, pp. 248–262.
[58] Cretaceous biostratigraphy and paleogeography of North Egypt and Northeast Libya; Pet. Res. J. 7 (1995) 75–93.
[59] Jurassic Prospects in the Western Desert, Egypt; 4th Petroleum Exploration Seminar, EGPC, Cairo, 1974, 20 p.
[60] Pyrolysis of Lower Cretaceous Matruh Shales, Mersa Matruh Well No. 1 Western Desert, Egypt; MERC Ain Shams Univ., Earth Sci. Ser., vol. 5, 1991, pp. 171–180.
[61] Cretaceous source rocks at Abu Gharadig oil and gas field Northern Western Desert, Egypt; J. Pet. Geol., England, 22 (4) (1999) 377–395.
[62] Physiochemical Characterization of Kerogen from Jurassic Shales in Well Mamura-1, Northwestern Egypt; Annals of the Geological Survey of Egypt, V.XXIII, 2000a, pp. 341–353.
[63] The Petroleum-Bearing Sections in the Western Desert: Cycles of Petroleum Generation, Migration and Accumulation Concepts and the Problem of Source-Reservoir Relation; A Review Article, The Supreme Permanent Scientific Committee (Geology for Promotion of the Professor Degree, Geology Department, Faculty of Science, Cairo Univ., April 2000, 2000b, 101 p.
[64] Paleotectonical Conditions Governed Formation of Oil and Gas Fields in the Northern Western Desert, Egypt (Ph.D. thesis), Fac. Geol., Moscow State Univ., Moscow, Russia (in Russian), 1983, 193 p.
[65] Implication of Elements of the Petroleum System and Reservoir Properties of Jurassic Lower Safa "C" in JG Field Area, Abu Gharadig Basin, North Western desert, Egypt, Egypt. J. Appl. Geophys. Egypt. Soc. Appl. Petrophys. (ESAP) 14, 2015.
[66] Basins Geometry and Tectonic Origin of the Desert of Egypt, Relevance to Economic Resources Fifth international Conference of Geology (GAW), Cairo Univ., Cairo, 2000.
[67] Hydrocarbon Source Rock Potentiality of Cretaceous Sediments in Abu Gharadig Basin, North Western Desert, Egypt (M.Sc. thesis), Geology Department, Faculty of Science, Al-Azhar Univ., Cairo, 2006, 189 p.
[68] Facies Models of a fine-grained, tide dominated delta; Lower Dir Abu Lifa Member (Eocene), Western Desert, Egypt, 2013.
[69] Fluvial to tidal transition zone facies in the McMurray Formation (Christina River, Alberta, Canada), with emphasis on the reflection of flow intensity in bottomset architecture, Elsevier Journal, 2011.
[70] Structural Geophysical Interpretation Basement Rocks of the North Western Desert of Egypt, Seminar on African Geology, Cairo, Egypt, 1979.
[71] Regional Structural Setting of Northern Egypt, 6th Exploration Seminar, EGPC, Cairo, 1982.
[72] Tectonic Framework, in: Said, R. (Ed.), The Geology of Egypt, Balkema, Rotterdam, 1990, pp. 113–155.
[73] Tectonic evaluation of the Abu Gharadig Basin, AAPG, Mediterranean Basins conference, Nice, France (Abstract), 1988.
[74] Reported folding and its significance in Northern Western Desert Petroleum Province; Arab Republic of Egypt, Acta Geologica Polonica, 29 (1) (1979) 133–150.
[75] New Lights on Hydrodynamic Type of Oil Field in the Western Desert of Egypt; 3rd Conference Arab World (GAW), Cairo Univ., Cairo, 1996, pp. 575–594.
[76] Pervasive E-ENE Oriented Faults in the Northern Egypt and Their Relationship to Late Cretaceous Petroliferous Basins in the Northern Western Desert, Egypt, in: Proc. 9th EGPC Petroleum Exploration and Production Conference, 1, 1988, pp. 51–67.
[77] Qarun Oil Field, Western Desert, Egypt, in: Proc. 13th EGPC Petroleum Exploration and Production Conference, 1, 1996, pp. 140–164.
[78] Rock Stratigraphic Nomenclature of the Western Desert; GUPCO, Cairo, Exploration Report No. 41, Pan Am. UAR Oil Company, (Unpublished Report, ER.557), 1967, 18 p.
[79] Summary of Source Rock and Crude Oil Analyses in the Western Desert, Egypt; Exploration Report no. 14, Gupco, Cairo, 1975.
[80] Tectonic Framework of Northern Egypt and the Eastern Mediterranean Region; 6th Exploration Seminar, EGPC, Cairo, 1982.
[81] Hydrocarbon Habitat of the western Desert, Egypt, in: 6th Exploration Seminar, EGPC, Cairo, 1982.
[82] Early Cretaceous Angiosperm Pollen from the Borehole Sedimentology, Can. Soc. Pet. Geol. Memoir (1991) 3–28.
[83] Cretaceous Sandstones as Oil and Gas Reservoirs and their Petrographic Characteristics in Northern Western Desert, Arab Republic of Egypt; 6 (1) (1980).
[84] Palynological Results and their Bearing on the Theory of Continental Displacement, Adv. Pollen-Spore Res., 1 (1974) 70–77.
[85] Palynological Studies in the Egyptian Western Desert, Umbarka IX Borehole; Pollen Spores, vol. 20, Paper No. 2, 1978, pp. 261–301.
[86] The Geology of Egypt; Elsevier Publ. Co., Amsterdam, 1962, 370 p.
[87] The Geology of Egypt, 1960.
[88] Nonmarine cretaceous correlations in Egypt and Northern Sudan; palynological and paleobotanical evidence, Cretaceous Res. 13 (1992) 351–368.
[89] Cretaceous (Aptian-Maastrichtian) Palynology of Foraminifera Dated Wells (KRM-1, AG-18) in Northwestern Egypt, with Notes on Eocene Dinoflagellates; Berliner Geowissenschaftliche Abhandlungen, 1995, pp. 1–44.
[90] Uber Die Kreideregion Bei Den Pyramiden Von Gizeh; Petrm. Mitth, Gotha, German, 1889, 35 p.
[91] Diagnostic attributes of clastic tidal deposits: a review, in: D.G. Smith, G.E. Reinson, B.A. Zaitlin, R.A. Rahmani (Eds.), 1991.
[92] Cimmeride Orogenic System and the Tectonics of Eurasia (special paper (Geological Society of America)), 1985.

[93] Quantitative Evaluation and Timing of Petroleum Generation in Abu Gharadig Basin, Western Desert, Egypt, in: 8th Petroleum Exploration Seminar, EGPC, Cairo, 1986, pp. 269–287.
[94] New Light on the Structural Development of the Western Desert of Egypt; Bull. Inst. Desert Egypt, vol. 3, Paper No. 1, 1953, pp. 101–106.
[95] Crude Oil Classification and Maturation of Abu Gharadig Basin, Western Desert, Egypt, Bull. Fac. Sci. Zagazig Univ., 1, 13, 1991, pp. 56–75.
[96] Depositional Environment of shallow marine sandstones from outcrop gamma-Ray logs, Belait formation, Meragang Beach, Brunei Darussalam, 2013, p. 309.
[97] Mid-Cretaceous Plant Microfossils from the Northern Part of the Western Desert of Egypt, Rev. Palaeobot. Palynol. 25 (1978) 259–267.
[98] Palynological Studies in the Nubia Sandstone Formation, East of Aswan, Southern Egypt, Neues Jahrbuch Geologic Palaeontologie Monatshefte, Vol. 10, 1985a, pp. 605–617.
[99] Maastrichtan Plant Microfossils from the El Mahamid Area, Nile Valley, Southern Egypt, Revue Micropaleon Tologie, Vol. 28, Paper No. 3, 1985b, pp. 213–222.
[100] Palynostratigraphy of Lower Cretaceous Sediments in the Nile Delta Region, Egypt, Revista Espanola Micropaleon tologia, Vol. 18, Paper No. 1, 1986, pp. 55–70.
[101] Palynological Zonation of Albian Cenomanian Sediments in the Northern Part of the Western Desert of Egypt, Bull. Faculty of Science, Alexandria University, Vol. 26, Paper No. 3, 1986, pp. 80–101.
[102] Palynostratigraphy of the Turonian-Lower Senonian Sequence, Gulf of Suez Area, Egypt, Bull. Faculty of Science, Alexandria University, Vol. 26, Paper No. 3, 1986, pp. l-17.
[103] Palynology of Albian-Cenomanian Strata in Mersa Matruh Well, Western Desert, Egypt, J. Afr. Earth Sci., Vol. 6, Paper No. 5, 1987, pp. 665–675.
[104] Tectonic Framework of Northern Western Desert, Egypt and its Effect on Hydrocarbon Accumulations, in: Proc. 9th EGPC Petroleum Exploration and Production Conference, 2, pp. 1988, 1–22.
[105] Mesozoic Rift Basins in Egypt, Their Southern Extension and Impact on Future Exploration, in: Proc. 11th EGPC Petroleum Exploration and Production Conference, 2, 1992, pp. 1–19.
[106] Facies Models Response to Sea Level Change, 1992, p. 179–217.
[107] Structural Pattern of Egypt and its Interpretation, Bull. AAPG 52 (1968) 601–614.
[108] On the Source Rock Possibilities of the Jurassic Sediments, Western Desert, Egypt, in: 8th JGES Hannover Abstract (page 106), 1980.
[109] Subsurface Geochemical Study in the Central Part of the Northern Western Desert, Egypt; Qatar Univ. Bull., 3, 1983, pp. 207–215.

Please cite this article in press as: H. Salama et al., Identify re-development concepts to enhance Abu Roash "C" oil reservoir productivity Sitra Area, Abu Gharadig Basin, Western Desert, Egypt, Egypt. J. Petrol. (2016), http://dx.doi.org/10.1016/j.ejpe.2016.04.003